Precambrian Research 390 (2023) 107046

Contents lists available at ScienceDirect

Precambrian Research

journal homepage: www.elsevier.com/locate/precamres

New evidence for the Baltican cratonic affinity and Tonian to Ediacaran tectonic evolution of West Avalonia in the Avalon Peninsula, Newfoundland, Canada

Luke P. Beranek [a,*], Alexander D. Hutter [a], Stephen Pearcey [a], Corey James [a], Vanessa Langor [a], Calum Pike [a], Dylan Goudie [b], Lindsay Oldham [a]

[a] Department of Earth Sciences, Memorial University of Newfoundland, 9 Arctic Avenue, St. John's, Newfoundland and Labrador, A1B 3X5 Canada
[b] Core Research Equipment and Instrument Training Network, Memorial University of Newfoundland, St. John's, Newfoundland and Labrador, A1C 5S7 Canada

ARTICLE INFO

Keywords:
Detrital zircon
Provenance
Avalonia
Neoproterozoic
Appalachians
Geochronology

ABSTRACT

Provenance studies of quartzite clasts and enclosing sandstone units in the Avalon Peninsula, Newfoundland, Canada, were conducted to test the Baltican or Gondwanan cratonic affinities of West Avalonia and examine the stratigraphic archives of Neoproterozoic arc evolution. Four cobble-sized quartzite clasts from a syn-orogenic, Ediacaran fluvial unit mostly yield ca. 1220, 1510, and 1900–2200 Ma detrital zircon age maxima and were probably derived from sub-arc basement units. Detrital zircon U-Pb-Hf isotope statistical assessments of the clasts indicate provenance ties with Proterozoic strata of the Sarmatian craton and Timanian passive margin of northern Fennoscandia, which corroborates models for proto-Avalonia to have originated near southern or northeastern Baltica, respectively. Analogous quartzite basement units in Nova Scotia and New England also have Baltican cratonic affinities and reflect provenance from southern Fennoscandia. Ediacaran exhumation of arc and basement infrastructure was accommodated by transpressive faults during the Avalonian orogeny and resulted in the deposition of Signal Hill Group terrestrial strata. Eleven Signal Hill Group sandstone samples are correspondingly dominated by Tonian to Ediacaran detrital zircon age fractions that constrain the crustal evolution of West Avalonia. The composite dataset includes 818–777 Ma detrital zircon grains that record the rifting of a proto-Avalonia sliver or ribbon arc from Baltica. Tonian igneous rocks are rare in West Avalonia, but ca. 760 Ma and 730 Ma detrital zircon grains indicate both crust and mantle contributions to the oceanic Burin arc, its tectonic interactions with proto-Avalonia, and subsequent arc magmatism across the composite terrane. Cryogenian detrital zircon ages substantiate the timing of 700–670 Ma magmatism and 670–640 Ma tectonic interactions with Baltica or another block. The detrital zircon U-Pb-Hf isotope record of the 640–600 Ma magmatic phase includes 6–9 Myr-long, fluctuating cycles that indicate the frequency of West Avalonian arc processes in the Mirovoi Ocean prior to Avalonian orogenesis.

1. Introduction

Avalonia is one of the largest superterranes in the Appalachian-Caledonian-Variscan mountain system of North America, Europe, and NW Africa (Fig. 1A). West Avalonia is exposed in the outboard parts of the northern U.S. and Canadian Appalachian orogen (Fig. 1B) and its exotic origin and displacement history have long been the subjects of debate (e.g., Williams, 1979; Keppie, 1985; Landing, 1996; van Staal et al., 1998; Waldron et al., 2014; Murphy et al., 2023). Much of the controversy has centered on its early arc development and disputed Cryogenian to Ediacaran plate tectonic interactions with the Baltican, West African, or Amazonian cratons (e.g., Murphy et al., 2004; van Staal et al., 2009; 2021a, 2021b; Henderson et al., 2016; Landing et al., 2022; all ages follow Cohen et al., 2013, v. 2022/10). Avalonia is a composite terrane defined by latest Ediacaran to Ordovician overstep sequence that covers its basement collage and may vary by location (e.g., Keppie, 1985; Landing, 1996). In general, four scenarios have been proposed to explain the tectonomagmatic evolution and Neoproterozoic paleogeography of West Avalonia and its basement assemblages (Murphy et al., 2023). The first scenario calls for Tonian to Cryogenian (ca. 730–650

* Corresponding author.
E-mail address: lberanek@mun.ca (L.P. Beranek).

https://doi.org/10.1016/j.precamres.2023.107046
Received 9 February 2023; Received in revised form 31 March 2023; Accepted 3 April 2023
0301-9268/© 2023 Elsevier B.V. All rights reserved.

Ma) development of a juvenile arc built on Mesoproterozoic crust, Cryogenian (ca. 665–650 Ma) accretion of the arc to the Amazonian margin of West Gondwana, late Cryogenian to Ediacaran (ca. 640–570 Ma) continental arc magmatism, and late Ediacaran (ca. 590–540 Ma) termination of subduction and transpressional deformation associated with the Avalonian orogeny, which may have resulted from ridge-trench collision and propagation of a San Andreas-style transform fault (e.g., Murphy and Nance, 1989; Murphy et al. 1999; Nance et al., 2002, 2008). The second scenario incorporates many features of the first model but considers that 730–650 Ma arc successions are underlain by slivers of Baltican crust (e.g., Henderson et al., 2016; Murphy et al., 2019). Both the first and second scenarios allow for West Avalonian basins to have sediment inputs from the Amazonian craton after arc-collision (e.g., Satkoski et al., 2010; Willner et al., 2013). The third scenario includes the generation of a 750–730 Ma arc built on a Baltican-derived ribbon, 700–670 Ma arc magmatism and collision with southern Baltica or another buoyant tectonic element, 640–560 Ma arc magmatism, and late Ediacaran arc-arc collision and strike-slip slivering with Ganderia along the Amazonian margin (van Staal et al., 2021a; Pollock et al., 2022; Thompson et al., 2022). In the third model, Ganderia was in the upper-plate of the arc-arc collision and shed quartzite clasts, garnet, and muscovite into West Avalonian basins during the Avalonian orogeny (van Staal et al., 2021a). The fourth scenario proposes that Avalonia is a microcontinent of Baltican cratonic affinity which separated from the Timanian margin of NE Baltica during the late Ediacaran (e.g., Landing, 1996; Keppie and Keppie, 2014; Landing et al., 2022).

The Avalon Peninsula of eastern Newfoundland is the type area for West Avalonia (Fig. 2, Avalon zone of Williams, 1979), but gaps in regional knowledge, especially the significance of Ediacaran strata that are linked to the Avalonian orogeny (Anderson et al., 1975; Mills et al., 2021), have hindered understanding of its Neoproterozoic tectonic evolution and paleogeography. van Staal et al. (2021a) highlighted the need to examine the overall stratigraphic and tectonic complexities of eastern Newfoundland and better correlate its geological history with West Avalonia units elsewhere in the Appalachians. Zircon U-Pb and Hf isotope studies have been particularly useful to test and develop plate tectonic scenarios for West Avalonia, including its long-term arc evolution (e.g., Pollock et al., 2015, 2022) and the Gondwanan or Baltican cratonic affinities of basement rocks in the U.S. (Kuiper et al., 2022; Severson et al., 2022; Thompson et al., 2022) and Canada (e.g., Barr et al., 2003; Satkoski et al., 2010; Henderson et al., 2016). Ediacaran strata in the Avalon Peninsula similarly have the potential to test West Avalonia tectonic evolution and include the Conception, St. John's, and Signal Hill Groups (Fig. 3). Signal Hill Group units record the erosion of arc infrastructure during the Avalonian orogeny and locally contain quartzite clasts and metamorphic minerals whose source is unknown (King, 1990; Williams et al., 1995).

In this article, we combine new quantitative mineral and detrital zircon U-Pb-Hf isotope studies of Conception Group and Signal Hill Group rock units to test published plate tectonic scenarios for West Avalonia and examine the Tonian to Ediacaran crustal evolution of its arc system in eastern Newfoundland. Our tectonic analysis includes a statistical comparison of West Avalonia detrital zircon U-Pb-Hf isotope results with published reference frames using MATLAB software packages. The results constrain the maximum depositional ages of sampled strata and statistically evaluate the Baltican or Gondwanan cratonic affinities of quartzite clasts. Our findings also allow us to examine Ganderian or local basement origins for these quartzite clasts and relate the deposition of Signal Hill Group strata with late Ediacaran exhumation and Avalonian orogenesis.

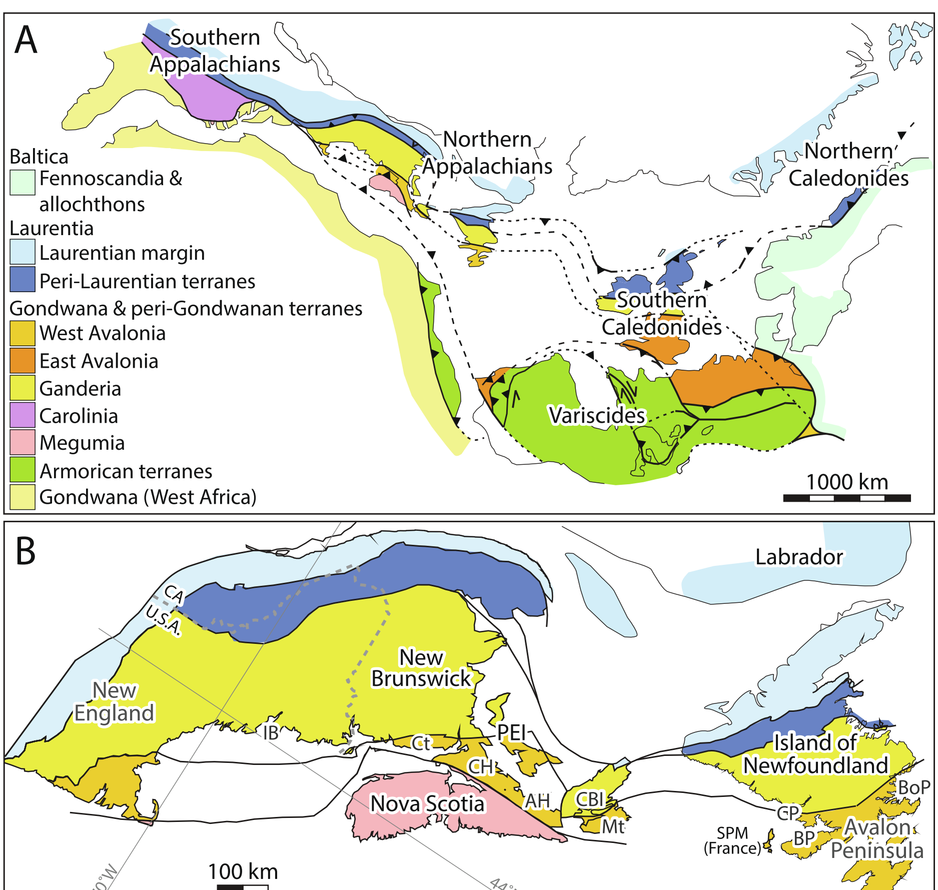

Fig. 1. (A) Pangean reconstruction of the Appalachian-Caledonian-Variscan orogenic belt modified from van Staal et al. (2021a). (B) Modern terrane map of the northern Appalachian orogen modified from Hibbard et al. (2006). AH - Antigonish Highlands; BoP - Bonavista Peninsula; BP - Burin Peninsula, CA - Canada; CBI - Cape Breton Island; CH - Cobequid Highlands; CP - Connaigre Peninsula; Ct - Caledonia terrane; IB- Islesboro block; Mt - Mira terrane; PEI - Prince Edward Island; SPM - Saint Pierre and Miquelon; U.S.A. - United States of America.

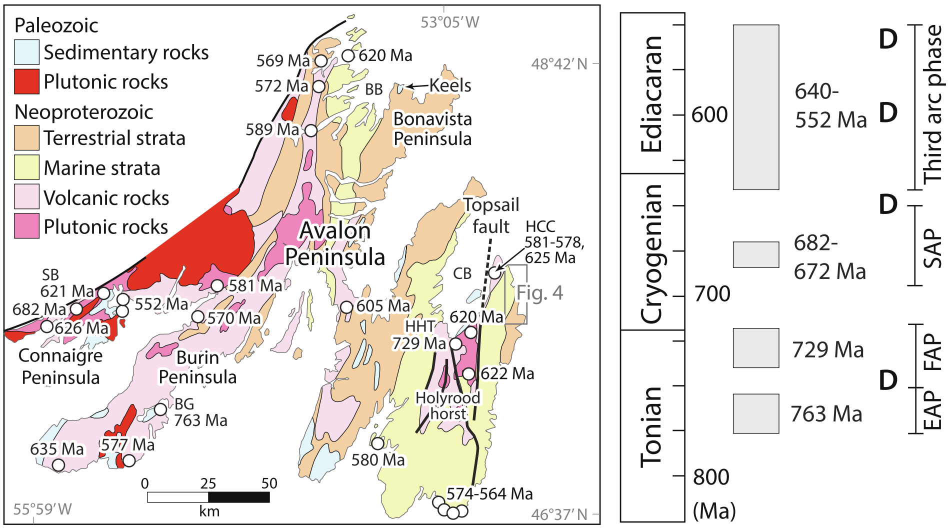

Fig. 2. Simplified Neoproterozoic to Paleozoic geology and magmatic evolution of the Avalon Peninsula region, eastern Newfoundland, modified from Colman-Sadd (1990), Pollock et al. (2015), and Mills et al. (2021). Quoted dates are representative zircon U-Pb crystallization ages for igneous rocks and depositional ages for tuffaceous rocks compiled from Israel (1998), Murphy et al. (2008), Skipton et al. (2013), Pu et al. (2016), Matthews et al. (2020), Mills et al. (2021), and references therein. Arc and deformational (D) phases from van Staal et al. (2021a). BB - Bonavista Bay; BG - Burin Group; CB - Conception Bay; EAP - Early arc phase; FAP - First arc phase; HCC - Horse Cove complex; HHT - Hawke Hills tuff; SAP - Second arc phase; SB - Simmons Brook Intrusive Suite.

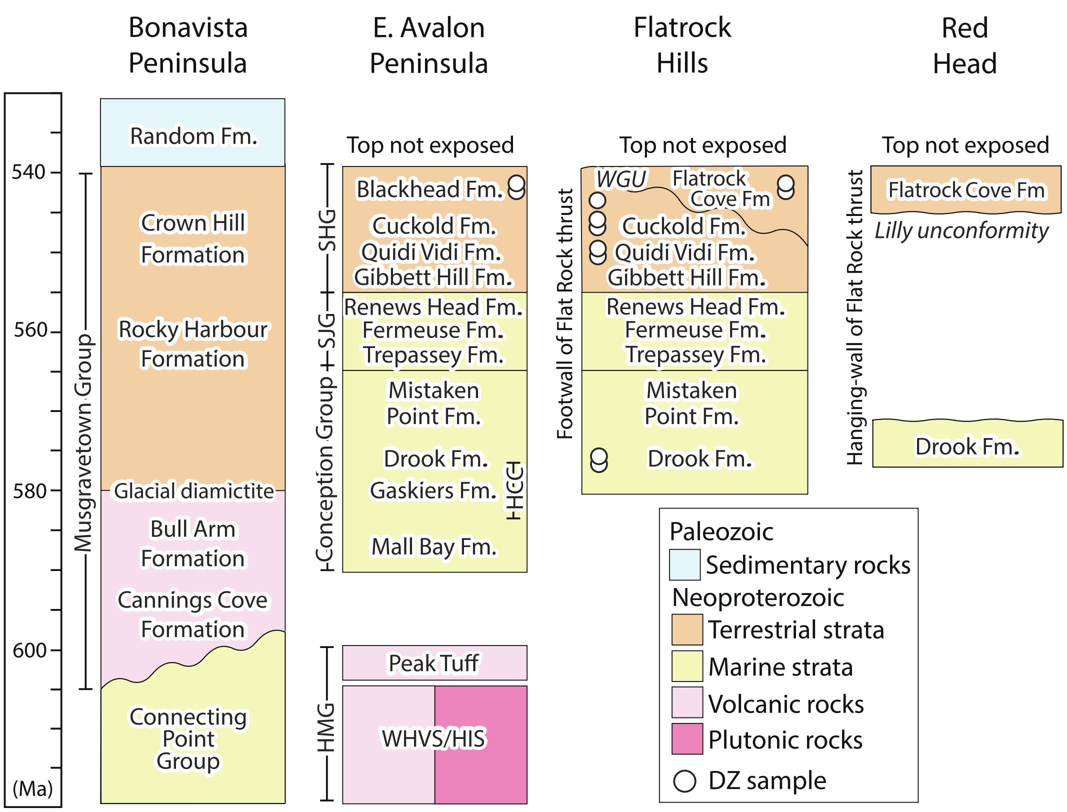

Fig. 3. Schematic lithostratigraphic columns for the Avalon Peninsula region modified from King (1990), Pollock et al. (2009), and Mills et al. (2021). Depositional ages of Signal Hill Group units are inferred from regional stratigraphic relationships and published zircon U-Pb results from Conception and St. John's Group rocks. Fm - Formation; HCC - Horse Cove complex; HMG - Harbour Main Group; SHG – Signal Hill Group; SJG – St. John's Group; WGU - Wind Gap unconformity; WHVS/HIS - White Mountains Volcanic Suite/Holyrood Intrusive Suite.

2. Geology of the Avalon Peninsula area, eastern Newfoundland

2.1. Tonian to Ediacaran arc and basin development

Tonian (765 ± 2 Ma, 763 ± 3 Ma) gabbro-quartz diorite-trondhjemite units and mafic flows of the Burin Group (BG in Fig. 2) are the oldest subduction-related rocks in West Avalonia and represent the vestiges of an intraoceanic arc system (e.g., Strong and Dostal, 1980; Krogh et al., 1988; Murphy et al., 2008a). Olistostromes that contain stromatolite-bearing carbonates are associated with the igneous rocks (O'Brien et al., 1996) and imply tectonic interactions between the Burin arc and a continental block (van Staal et al., 2021a). The oldest rocks in the NE Avalon Peninsula are 729 ± 2 Ma units of the Hawke Hills Tuff (HHT in Fig. 2; Israel, 1998). Basement to the Hawke Hills Tuff is not exposed, but the rocks may correlate with 750–730 Ma plutons that intrude metasedimentary assemblages in Nova Scotia (e.g., Doig et al., 1993; White et al., 2021).

Early Cryogenian arc magmatism is recorded by 682–672 Ma calc-alkaline rocks in the Connaigre Peninsula (Fig. 2, e.g., O'Brien et al., 1996). Broadly equivalent units in Cape Breton Island, Nova Scotia (CBI in Fig. 1B), include Stirling Group strata that contain Tonian to Neoarchean detrital zircon grains with εHf$_{(t)}$ values of +4.9 to −4.5 (Willner et al., 2013). Whole-rock and zircon isotope data further demonstrate Meso-to Paleoproterozoic crustal contributions to arc rocks (e.g., Murphy et al., 1999, 2000; Pollock et al., 2015, 2022). This arc phase was apparently followed by a 30 Myr gap in magmatism and pre-630 Ma deformation and high-grade metamorphism in Newfoundland (Fig. 2, O'Brien et al., 1996) and Cape Breton Island (Keppie et al., 1998). These events have been used to interpret the collision of the West Avalonian arc with Amazonia (Nance et al., 2002, 2008; Murphy et al., 2000, 2013) or Baltica (Thompson et al., 2012, 2022; van Staal et al., 2021a).

Cryogenian to Ediacaran (640–552 Ma) rocks intrude and overlie older arc elements from the Connaigre Peninsula to the Avalon Peninsula (Fig. 2). Ediacaran (ca. 620 Ma) rocks of the Simmons Brook intrusive suite (SB in Fig. 2) yield subchondritic zircon εHf$_{(t)}$ values that indicate the reworking of Tonian and older sub-arc crust (Pollock et al., 2015, 2022). Although most arc-proximal basin successions were sourced from igneous rocks, ca. 620–605 Ma Connecting Point Group strata of the Eastport basin near Bonavista Bay (BB in Fig. 2) contain garnet-mica schist fragments and detrital garnet (Dec et al., 1989, 1992). The top of the Connecting Point Group in the Bonavista Peninsula is marked by an angular unconformity (Fig. 3), implying that metamorphic detritus in the Eastport basin is linked to 605–600 Ma thrust faulting and tilting reported by Mills et al. (2016, 2021). Post-605 Ma rocks developed in an extensional arc regime (e.g., Murphy, 2002; Thompson et al., 2014; Mills et al., 2021), including ca. 580 Ma Horse Cove complex units (HHC in Figs. 2, 3; Skipton et al., 2013) that yield ca. 1378 Ma inherited zircon from sub-arc crust.

Conception, St. John's, and Signal Hill Group strata were deposited during the transition from arc activity to subduction termination, deformation, and exhumation of West Avalonia infrastructure (Fig. 4A, e.g., Myrow, 1995). Marine rock units of the 2.6 km-thick Conception Group, including Torbay and Bauline Line Member sediment gravity flows of the Drook Formation (Fig. 3), were deposited on arc successions (e.g., King, 1990; O'Brien et al., 2001) and contain 630–565 Ma detrital zircon grains with chondritic to superchondritic Hf isotope compositions (Pollock et al., 2009, 2015). Conception Group tuffs have precisely dated 574.17 ± 0.66 Ma to 565.00 ± 0.64 Ma fossil (Matthews et al., 2021) and 580.90 ± 0.40 Ma to 579.24 ± 0.17 Ma Gaskiers diamictite (Pu et al., 2016) horizons. Marine to deltaic strata of the St. John's Group, which are ~1 km-thick near St. John's, conformably overlie the Conception Group (e.g., King, 1990) and contain 564.71 ± 0.88 Ma and 564.13 ± 0.65 Ma tuffs (Matthews et al., 2021). The lower Signal Hill Group consists of the Gibbett Hill, Quidi Vidi, and Cuckold Formations and includes ~1.7 km of sandstone and conglomerate (Fig. 3; King, 1990). Basal Signal Hill Group strata contain detrital garnet and muscovite grains and imply that terrestrial deposition was linked to the uplift and erosion of metamorphic basement (Papezik, 1973). The 800 m-thick Cuckold Formation is divided into Cabot Tower, Cape Spear, and Skerries Bight Members that represent a braided fluvial system that drained to the south-southwest (King, 1990). Cape Spear Member units locally contain clasts of quartzite, and near Flatrock, ~20 km north of St. John's, are exposed in ~2 m-thick quartzite marker bed (Fig. 4B; Calon, 2005). Cape Spear Member quartzite clasts have been documented ~25 km south of Flatrock through the Torbay Point, Signal Hill, and Cape Bay areas (King, 1990).

The upper Signal Hill Group in the Flatrock area is represented by the 600 m-thick Flatrock Cove Formation (Figs. 3, 4B), which consists of Knobby Hill Member braided fluvial sandstone and conglomerate units with south-southwest-directed paleoflow indicators overlain by Piccos Brook Member alluvial fan sandstone and breccia units. Flatrock Cove Formation strata unconformably overlie upper Cuckold to lower Quidi Vidi Formation rocks in the Flatrock Hills (Fig. 5A; Wind Gap unconformity), which requires >500 m of erosion (King, 1990; Calon, 2005). The Flatrock Cove Formation consists of sediment wedges bounded by progressive, syn-tectonic unconformities that merge with this angular unconformity, consistent with most of the Knobby Hill and Piccos Brook Member rocks representing syn-growth strata deposited during regional

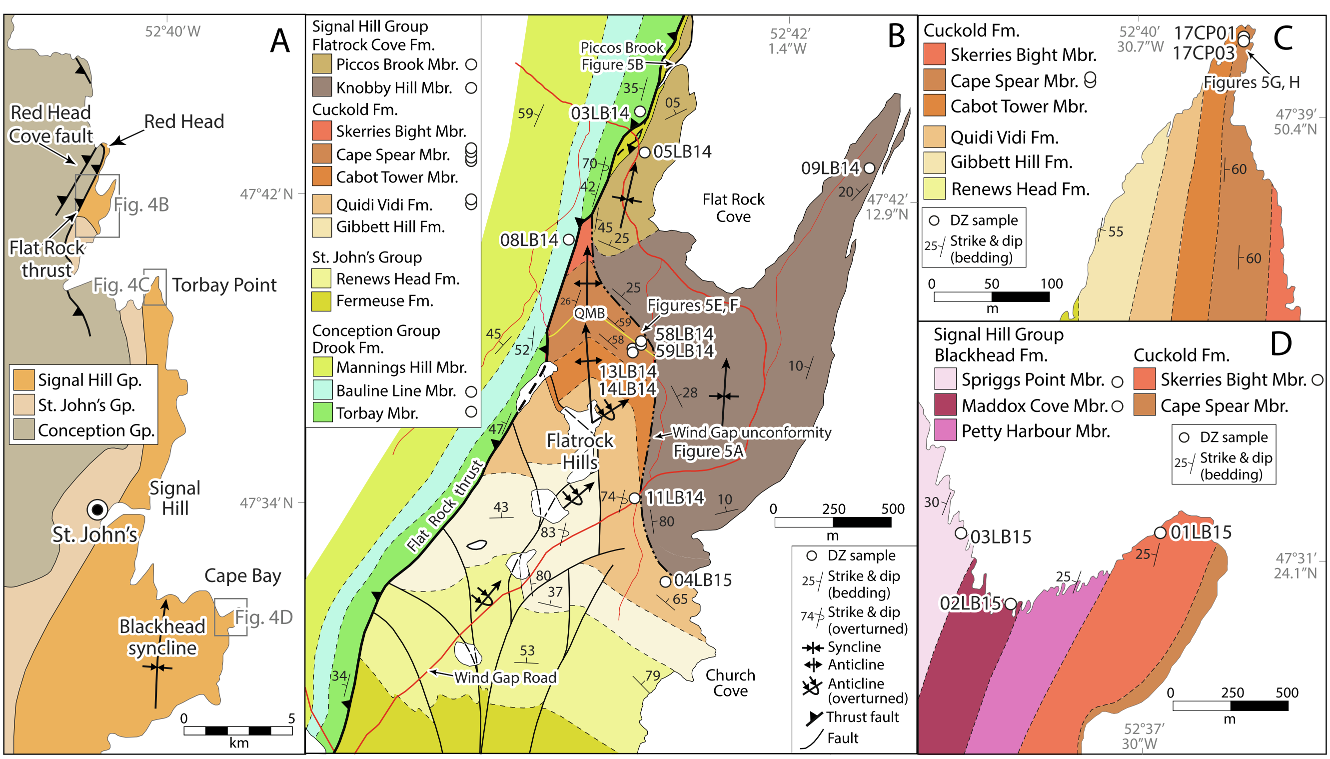

Fig. 4. Simplified Neoproterozoic geology of the (A) northeastern Avalon Peninsula; (B) Flatrock area; (C) Torbay Point area; and (D) Cape Bay area modified from Williams and King (1979), King (1990), and Calon (2005). Dashed lines are gradational or approximated contacts. Fm. - Formation; Gp. - Group; QMB - Quartzite Marker Bed; Mbr. - Member.

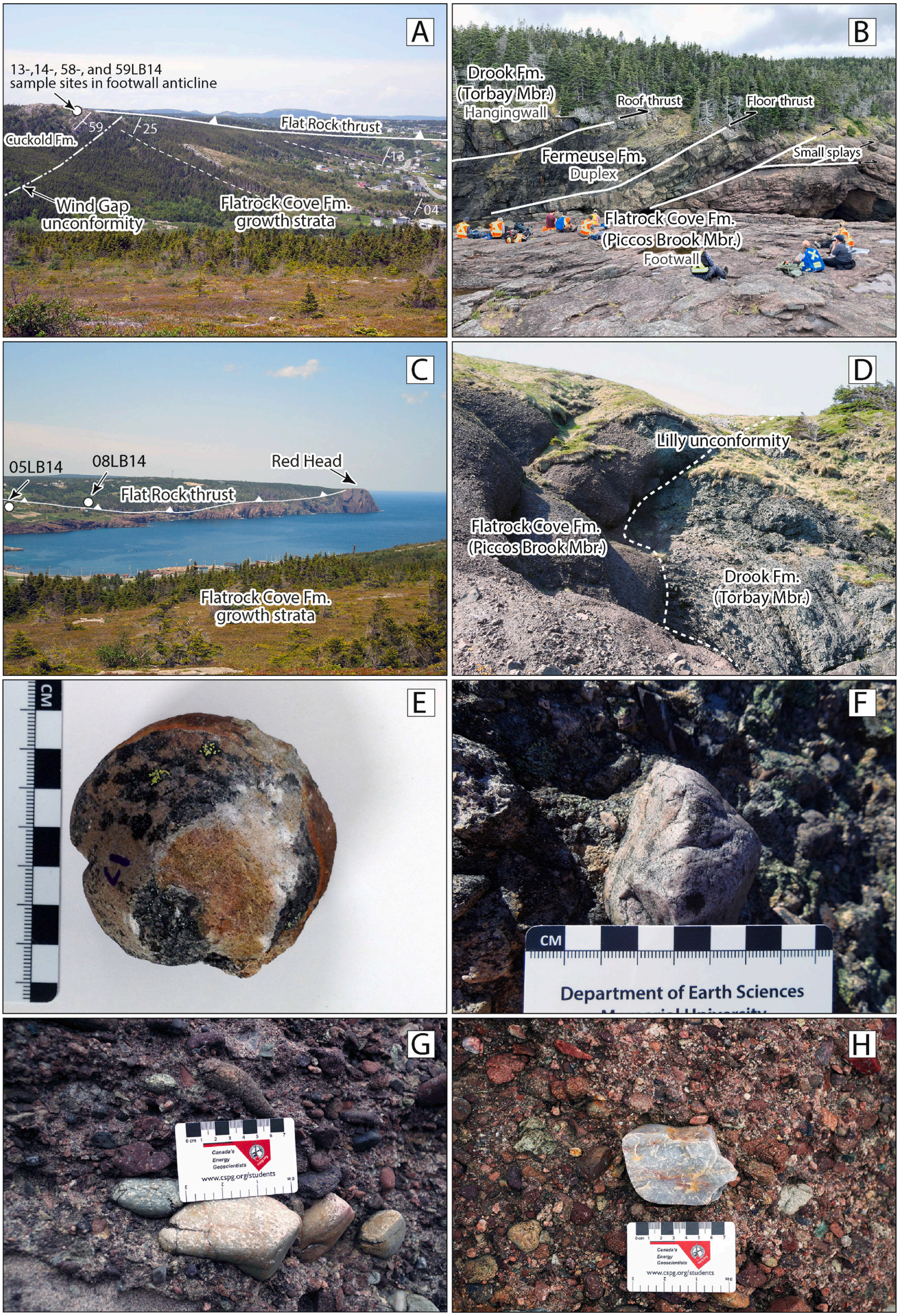

Fig. 5. (A) West-facing view of Flatrock Hills with Flatrock Cove Formation growth strata in the foreground that sit on Cuckold Formation and older rock units along the Wind Gap unconformity. Flat Rock thrust in background puts Conception Group rocks on top of Signal Hill Group rocks. Field of view ~1000 m. (B) North-facing view of Flat Rock thrust zone at the mouth of Piccos Brook. Field of view ~200 m. (C) Northwest-facing view of Flat Rock thrust along Flat Rock Cove to Red Head. Field of view ~1500 m. (D) Lilly unconformity at Red Head with Piccos Brook Member rocks sitting on folded Torbay Member rocks. (E) Sample 59LB14 and (F) Sample 58LB14 clast from quartzite marker bed in Flatrock Hills. (G) Sample 17CP03 and (H) Sample 17CP01 clasts from Torbay Point. (For interpretation of the references to colour in this figure legend, the reader is referred to the web version of this article.)

deformation (Calon, 2005). Upper Signal Hill Group strata along Cape Bay, ~8 km southeast of St. John's, comprise the ~1.7 km-thick Blackhead Formation that gradationally overlies the upper Cuckold Formation (Fig. 3; King, 1990). The Blackhead Formation has five members (Petty Harbour, Maddox Cove, Spriggs Point, Deadman's Brook, Cliff Point) that were parts of a south-southwest-directed braided fluvial system (King, 1990). The stratigraphic position of the Blackhead Formation relative to the Flatrock Cove Formation is uncertain.

2.2. Ediacaran deformation related to the Avalonian orogeny

Avalonian deformation in the NE Avalon Peninsula is best illustrated by Ediacaran strata involved in the Flat Rock thrust in Flatrock. The Flat Rock thrust is a dextral transpressive fault (Brubacher, 2016) and defined by Conception Group strata in the hanging-wall and Signal Hill Group strata in the footwall; a duplex of St. John's Group is locally exposed at Piccos Brook (Fig. 4B, 5B, 5C, Evans, 2010; Brubacher, 2016). There is an estimated 3.5 km of throw on the fault based on stratigraphic offsets (Williams and King, 1979; King, 1990; Calon, 2005). Lower Piccos Brook Member alluvial fan units are dominated by hanging-wall clasts sourced from the Drook Formation. Upper Piccos Brook Member strata at Red Head, ~1 km north of Piccos Brook, unconformably overlie folded Drook Formation strata (Fig. 4A, 5C, 5D, Lilly unconformity of Anderson et al., 1975). Field relationships at Red Head require alluvial fan rocks to comprise part of a wedge-top basin or that the age of the upper Piccos Brook Member post-dates the latest episode of Avalonian thrusting. Flatrock Cove Formation strata at Red Head are tilted (Anderson et al., 1975), but it is uncertain if this was related to Avalonian or mid-Paleozoic tectonic events.

The depositional ages of Signal Hill Group strata are unresolved, and as a result, the timing and duration of Avalonian deformation have remained elusive. Signal Hill Group strata lack fossils and tuffaceous units typical of underlying marine rocks. Blackhead and Flatrock Cove Formation strata have erosional tops and their original upper contacts are unknown (Fig. 3). Although the upper contact of the Signal Hill Group is not exposed in the NE Avalon Peninsula, Cambrian strata unconformably overlie tilted Conception Group rocks and nonconformably overlie Ediacaran granitoids ~40 km west of St. John's (e.g., Anderson, 1987). Farther west in the Bonavista Peninsula, Signal Hill Group equivalents are conformably overlain by Terreneuvian strata of the Random Formation near Keels (Figs. 2, 3, e.g., O'Brien and King, 2004). Avalonian deformation in the St. John's area has not been robustly dated, however, shear zone rocks that separate 625–620 Ma and 584 Ma intrusive-extrusive units in the Holyrood horst, which lies west of the Topsail fault (Fig. 2), yielded a preliminary sericite Ar-Ar age of 537 ± 3 Ma (Sparkes et al., 2021).

3. Materials and methods

3.1. Scanning Electron Microscopy – Mineral Liberation Analysis

Quantitative mineral studies of 12 thin sections were conducted using a FEI Quanta field emission gun 650 scanning electron microscope (SEM) equipped with Mineral Liberation Analysis (MLA) software version 3.14 (Table S1, e.g., Sylvester, 2012; Grant et al., 2018; Beranek et al., 2022). Instrument conditions included a high voltage of 25 kV, working distance of 13.5 mm, and beam current of 10nA. MLA maps (Figure S1) were created using GXMAP mode by acquiring Energy Dispersive X-ray spectra in a grid every 10 pixels, with a spectral dwell time of 12 ms, and comparing these against a list of mineral reference spectra. The MLA frames were 1.5 mm by 1.5 mm with a resolution of 500 pixels × 500 pixels. Table S1 reports area percentages for: (1) rock-forming minerals (feldspar, quartz); (2) accessory minerals (e.g., apatite, garnet); and (3) secondary minerals that result from low-grade metamorphism (Papezik, 1972, 1974; e.g., albite, ferriprehnite, phengite) or diagenesis (e.g., iron oxide). Muscovite exists as accessory and secondary phases and reported here in the latter group. Potassium feldspar values are the sum of orthoclase, microcline, and sanidine abundances in each sample.

3.2. Detrital zircon U-Pb geochronology and Hf isotope geochemistry

Sample preparation techniques, split-stream and conventional laser ablation methods (Fisher et al., 2014; Beranek et al., 2020), and results for 15 rock samples and reference materials are reported in Table S2. Time-integrated U-Pb analyte signals were analyzed offline using Iolite software, which includes a correction routine for down-hole fractionation (Paton et al., 2011). Age calculations were made using the VizualAge DRS (Petrus and Kamber, 2012). Concordance values were calculated as the ratio of $^{206}Pb/^{238}U$ and $^{207}Pb/^{206}Pb$ ages and analyses with high error (>10% uncertainty) or excessive discordance (>10% discordant, >5% reverse discordant) were excluded from maximum depositional age estimates and provenance interpretations. The reported ages for grains younger and older than 1200 Ma are based on $^{206}Pb/^{236}U$ and $^{207}Pb/^{206}Pb$ ages, respectively.

U-Pb dates are reported at 2σ uncertainty and presented in probability density plots made with the DZmnf MATLAB program of Saylor et al. (2019). Age maxima were determined with the AgeCalcML MATLAB program (https://github.com/kurtsundell/AgeCalcML). Initial $^{176}Hf/^{177}Hf$ ratios are reported as $\varepsilon Hf_{(t)}$ and represent isotopic compositions at the time of crystallization relative to the chondritic uniform reservoir (CHUR). Initial epsilon Hf ($\varepsilon Hf_{[t]}$) calculations used the decay constant of Söderlund et al. (2004) and CHUR values of Bouvier et al. (2008). $\varepsilon Hf_{(t)}$ vs U-Pb age plots were made with the Hafnium Plotter MATLAB program of Sundell et al. (2019). Maximum depositional ages were estimated with four methods: (1) the youngest single detrital zircon grain (YSG); (2) the youngest statistical peak (YSP) of Coutts et al. (2019), which takes a weighted mean of the youngest population of two or more grains that yield a MSWD ~1; (3) the youngest grain cluster (YGC2σ) of Dickinson and Gehrels (2009), which takes the weighted mean of the youngest three or more grains that overlap at 2σ; and (4) the Maximum Likelihood Age algorithm of Vermeesch (2021). U-Pb and U-Pb-Hf statistical assessments (Table S3) were conducted with the DZstats (Saylor and Sundell, 2016) and DZstats2D (Sundell and Saylor, 2021) MATLAB programs, respectively. Multi-dimensional scaling (MDS) plots were made with the DZmds (Saylor et al., 2018) and DZstats2D (Sundell and Saylor, 2021) MATLAB programs.

4. Results

4.1. Drook Formation

Torbay Member sandstone (03LB14 in Fig. 4B) has 34.27% quartz, 2.03% potassium feldspar, and 0.06% plagioclase (Table S1). Accessory minerals include allanite (0.08%), apatite (0.08%), and titanite (0.90%), and secondary mineral contents are dominated by albite (44.91%), chlorite (2.76%), ferriprehnite (0.24%), muscovite (5.66%), and phengite (5.22%). Torbay Member sandstone yields 572 ± 7 Ma to 744 ± 22 Ma detrital zircon grains with age maxima of 620 Ma and 628 Ma (Fig. 6, $n = 97/112$ indicates that 97 of 112 analyses passed discordance filter). Bauline Line Member breccia units contain clasts of felsic igneous rocks and a sample of sandy matrix (08LB14 in Fig. 4B) has 48.79% quartz, 2.58% potassium feldspar, and 0.04% plagioclase (Table S1). Accessory minerals include allanite (0.08%), apatite (0.06%), rutile (0.02%), and titanite (0.50%). The Bauline Line Member sample contains 562 ± 12 Ma to 655 ± 9 Ma detrital zircon grains with age maxima of 607 Ma and 617 Ma and single-grain ages of 673 Ma to 1257 Ma (Fig. 6, $n = 91/109$). Ediacaran to Cryogenian detrital zircons in the Torbay and Bauline Line Member samples have $\varepsilon Hf_{(t)}$ values of +9.8 to −4.2 ($\overline{X}$= +3.5) and +8.1 to −4.7 ($\overline{X}$= +2.9), respectively (Fig. 6). Single 759 ± 8 Ma and 1257 ± 36 Ma grains yield $\varepsilon Hf_{(t)}$ values of +3.9 and +6.1, respectively.

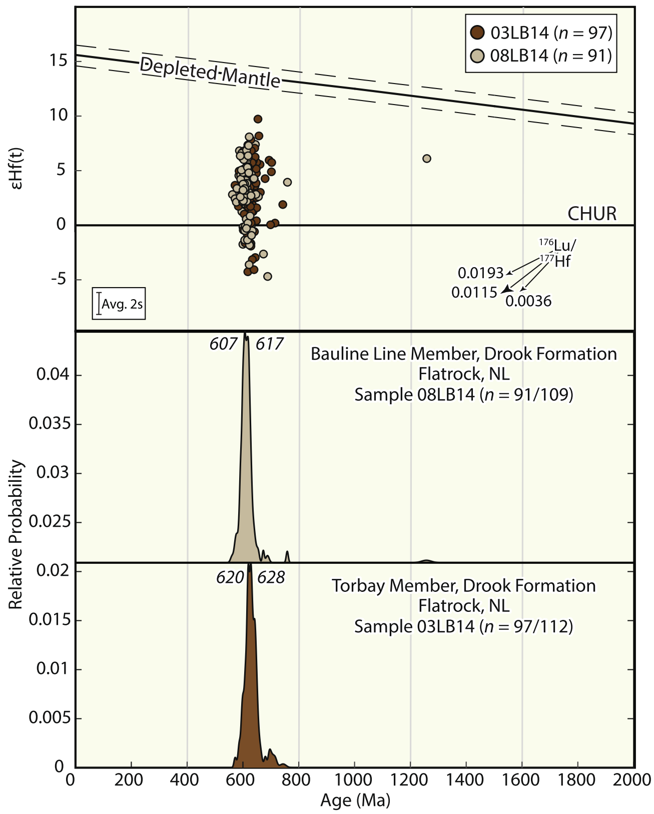

Fig. 6. Detrital zircon results from Conception Group rock units: Torbay Member sandstone, Drook Formation (sample 03LB14) and Bauline Line Member breccia matrix, Drook Formation (08LB14). CHUR is chondritic uniform reservoir. Crustal evolution trends show an average $^{176}Lu/^{177}Hf$ value of 0.0115 and a range of $^{176}Lu/^{177}Hf$ values of 0.0193 to 0.0036 (e.g., Vervoort et al., 1999). NL - Newfoundland and Labrador. n = number of grains that passed discordance filter against total number of analyses.

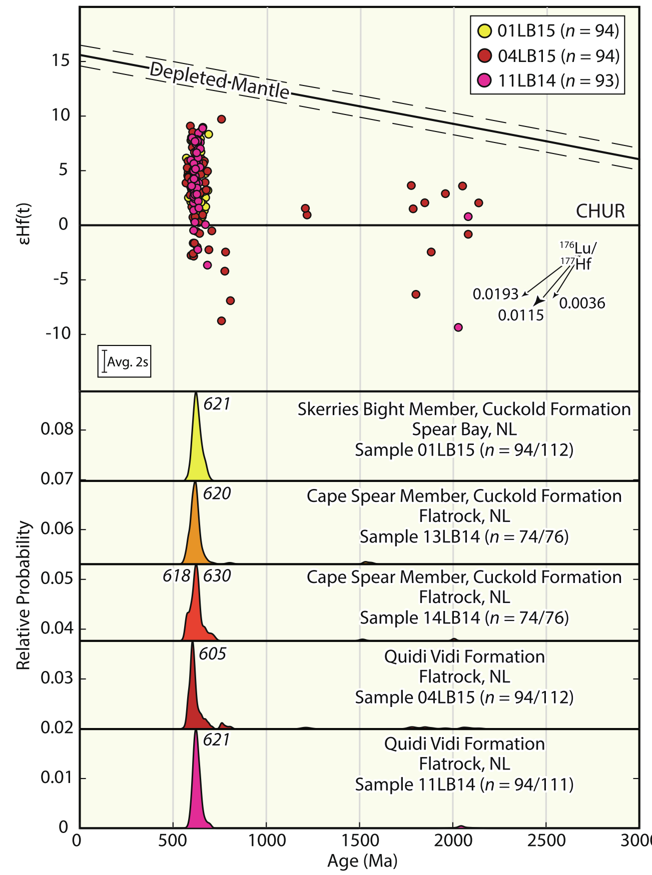

Fig. 7. Detrital zircon results from lower Signal Hill Group rock units: Quidi Vidi Formation (11LB14), Quidi Vidi Formation (04LB15), Cape Spear Member conglomerate matrix, Cuckold Formation (14LB14), Cape Spear Member conglomerate matrix, Cuckold Formation (13LB14), and Skerries Bight Member sandstone, Cuckold Formation (01LB15). CHUR is chondritic uniform reservoir. Crustal evolution trends show an average $^{176}Lu/^{177}Hf$ value of 0.0115 and a range of $^{176}Lu/^{177}Hf$ values of 0.0193 to 0.0036 (e.g., Vervoort et al., 1999). NL - Newfoundland and Labrador. n = number of grains that passed discordance filter against total number of analyses.

4.2. Quidi Vidi Formation

Quidi Vidi Formation sandstones along Wind Gap Road and Church Cove (11LB14 and 04LB15 in Fig. 4B) have 44.75% and 49.97% quartz, respectively, but the latter has 6 times more (7.99%) potassium feldspar (Table S1). Sample 11LB14 mostly has 596 ± 10 Ma to 699 ± 10 Ma detrital zircon grains with age maxima of 621 Ma (Fig. 7, n = 94/111). The sample has single grain ages of 2030 ± 44 Ma to 2083 ± 44 Ma. Sample 04LB15 mostly yields 570 ± 14 Ma to 708 ± 9 Ma grains with age maxima of 605 Ma (Fig. 7, n = 94/112). Five grains comprise an age fraction of 760 ± 8 Ma to 808 ± 11 Ma. The sample includes single grains of 1210 Ma to 2139 Ma (Fig. 7). Ediacaran to Cryogenian detrital zircon grains in the Wind Gap Road and Church Cove samples have $\varepsilon Hf_{(t)}$ values of +8.9 to −3.7 ($\overline{X}$= +4.6) and +9.1 to −2.8 ($\overline{X}$= +3.9), respectively (Fig. 7). The 808–760 Ma age fraction yields $\varepsilon Hf_{(t)}$ values of +9.7 to −8.8 ($\overline{X}$ = -2.5), whereas Stenian to Ectasian and Rhyacian age groups have $\varepsilon Hf_{(t)}$ values of +1.0 to +1.6 ($\overline{X}$= +1.3) and +3.6 to −6.3 ($\overline{X}$= +0.7), respectively (Fig. 7).

4.3. Cuckold Formation

Cape Spear Member conglomerate units are dominated rhyolite porphyry and granite clasts (Table S4). Sandy matrix was collected from two Cape Spear Member conglomerate units in the Flatrock Hills (Fig. 4B). A lower sample ~10 m beneath the quartzite marker bed (14LB14) has 42.92% quartz, 10.55% potassium feldspar, and 0.01% plagioclase (Table S1). The accessory mineral abundance is mostly controlled by titanite (0.10%); the sample also has trace (<0.01%) garnet. Sample 14LB14 mostly yields 565 ± 11 Ma to 681 ± 13 Ma detrital zircon grains with age maxima of 618 Ma and 630 Ma (Fig. 7, n = 74/76). The lower sample includes single grain ages of 708 ± 17 Ma to 1561 ± 17 Ma. An upper sample (13LB14) at the base of the marker bed yields 560 ± 8 Ma to 721 ± 13 Ma detrital zircon grains with age maxima of 620 Ma (Fig. 7, n = 74/76). The upper sample includes single grain ages of 1516 ± 17 Ma and 2007 ± 12 Ma.

Two quartzite clasts were collected in the Flatrock Hills. A tan, subrounded, cobble-sized clast of subfeldspathic metasandstone (59LB14 in Fig. 4B, Fig. 5E) mostly yields 1554 ± 21 Ma to 1599 ± 58 Ma, 1823 ± 50 Ma to 2196 ± 56 Ma, and 2413 ± 41 Ma to 2896 ± 29 Ma detrital zircon grains with major age maxima of 1981 Ma and lesser maxima of 1564 Ma and 2757 Ma (Fig. 8, n = 120/124). The sample includes single grain ages of 606 ± 12 Ma to 3080 ± 19 Ma. Detrital zircon grains that comprise the 1981 Ma age maxima yield $\varepsilon Hf_{(t)}$ values (Fig. 8) of +9.1 to −7.5 ($\overline{X}$= +1.8). Detrital zircons that comprise the 1564 Ma and 2757 Ma age maxima have $\varepsilon Hf_{(t)}$ values of −0.2 to −2.8 ($\overline{X}$ = −1.5) and +1.3 to −6.5 ($\overline{X}$ = −2.2), respectively (Fig. 8). A pink, subrounded to rounded, cobble-sized clast of quartz metasandstone (58LB14 in Fig. 4B, Fig. 5F) yields 1115 ± 12 Ma to 1257 ± 26 Ma, 1349 ± 38 Ma to 1578 ± 28 Ma, 1754 ± 22 Ma to 1913 ± 22 Ma, 1950 ± 28 Ma to 2150 ± 21 Ma, 2488 ± 11 Ma to 2884 ± 16 Ma, and 2942 ± 18 Ma to 3054 ± 21 Ma detrital zircon grains with major age maxima of

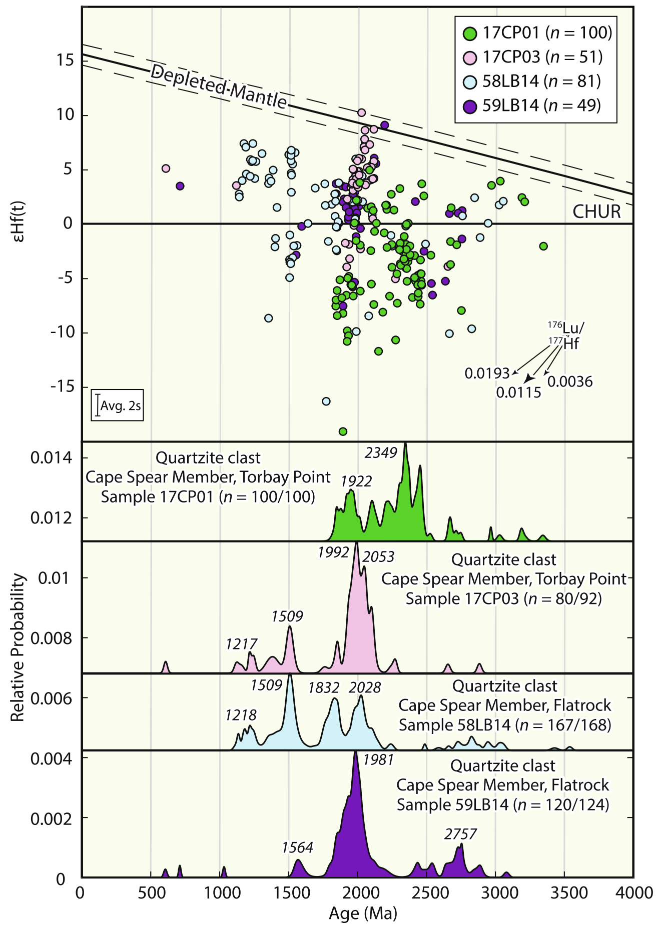

Fig. 8. Detrital zircon results from Cape Spear Member quartzite clasts: Flatrock subfeldspathic metasandstone (59LB14), Flatrock quartz metasandstone (58LB14), Torbay Point micaceous quartz metasandstone (17CP03), and Torbay Point quartz metasandstone (17CP01). See text and Fig. 5E-5H for supporting information. CHUR is chondritic uniform reservoir. Crustal evolution trends show an average ^{176}Lu/^{177}Hf value of 0.0115 and a range of ^{176}Lu/^{177}Hf values of 0.0193 to 0.0036 (e.g., Vervoort et al., 1999). n = number of grains that passed discordance filter against total number of analyses.

1509, 1832, and 2028 Ma and lesser age maxima of 1136, 1186, and 1218 Ma (Fig. 8, n = 167/168). The sample has single grain ages of 3429 ± 27 Ma and 3539 ± 19 Ma. Detrital zircon grains that comprise the 1509, 1832, and 2028 Ma age maxima yield εHf$_{(t)}$ values of +6.8 to −4.9 ($\overline{X}$= +1.6), +3.8 to −16.3 ($\overline{X}$ = −0.5), and +6.0 to −9.9 ($\overline{X}$= +1.1), respectively (Fig. 8). Detrital zircon grains that form the 1136–1218 Ma age maxima and 2661–3052 Ma age fraction have εHf$_{(t)}$ values of +7.4 to +2.5 ($\overline{X}$= +5.2) and +2.1 to −10.1 ($\overline{X}$ = −1.7), respectively.

Two quartzite clasts were collected from the quartzite marker bed at Torbay Point (Fig. 4C, 5G, 5H). Sample 17CP03 is a grey, subrounded to subangular, cobble-sized clast with 84.56% quartz, 9.29% potassium feldspar, 5.95% muscovite, and 0.11% apatite (Table S1). Sample 17CP03 yields 1121 ± 16 Ma to 1250 ± 14 Ma, 1349 ± 36 Ma to 1515 ± 19 Ma, and 1840 ± 21 Ma to 2118 ± 20 Ma detrital zircon grains with major age maxima of 1992 Ma and 2053 Ma and lesser maxima of 1217 Ma and 1509 Ma (Fig. 8, n = 80/92). The sample includes single grain ages of 608 ± 13 Ma to 2884 ± 16 Ma. Detrital zircon grains that comprise the 1992 Ma and 2013 Ma age maxima yield εHf$_{(t)}$ values of +10.2 to −5.0 ($\overline{X}$= +3.8) and a single 1121 ± 16 Ma grain has an εHf$_{(t)}$ value of +3.5 (Fig. 8). Sample 17CP01 is a grey, subrounded, cobble-sized clast with 97.99% quartz, 1.86% muscovite, 0.02% potassium feldspar, and 0.01% zircon (Table S1). Sample 17CP01 yields 1837 ± 14 Ma to 2476 ± 13 Ma and 2669 ± 15 Ma to 2748 ± 14 Ma detrital zircon grains with major age maxima of 1922 Ma and 2349 Ma and lesser age maxima of 1846, 2049, 2207, 2302, 2456, and 2672 Ma (Fig. 8, n = 100/100). The sample includes single grain ages of 2967 ± 8 Ma to 3344 ± 20 Ma. Detrital zircon grains that make up the 1846–2456 Ma age maxima and >2672 Ma age fraction yield εHf$_{(t)}$ values of +5.1 to −19.0 ($\overline{X}$ = −3.6) and +4.1 to −7.8, respectively (Fig. 8).

Skerries Bight Member conglomerate along Cape Bay contains clasts of rhyolite porphyry and granite (Table S4). Skerries Bight Member sandstone (01LB15 in Fig. 4D) yields 48.73% quartz, 8.00% potassium feldspar, and 0.02% plagioclase (Table S1). Accessory mineral contents include allanite (0.04%), apatite (0.04%), ilmenite (0.02%), and titanite (0.48%). Sample 01LB15 yields 575 ± 7 Ma to 694 ± 12 Ma detrital zircon grains with age maxima of 621 Ma (Fig. 7, n = 94/112). Ediacaran to Cryogenian detrital zircon grains have εHf$_{(t)}$ values of +9.0 to + 0.4 ($\overline{X}$= +4.9).

4.4. Flatrock Cove Formation

Knobby Hill Member sandstone (09LB14 in Fig. 4B) yields 41.40% quartz, 13.73% potassium feldspar, and (<0.01%) plagioclase, and accessory minerals that include allanite (0.03%), apatite (0.04%), garnet (0.01%), rutile (0.01%), and titanite (0.46%) (Table S1). Knobby Hill Member sandstone mostly yields 617 ± 8 Ma to 778 ± 21 Ma detrital zircon grains with age maxima of 619 Ma (Fig. 9, n = 24/25). The sample includes 1150 ± 17 Ma to 2127 ± 30 Ma single grain ages. Piccos Brook Member sandstone (05LB14 in Fig. 4B) has 54.42% quartz, 0.93% potassium feldspar, and 0.20% plagioclase, and accessory minerals that include allanite (0.03%), apatite (0.02%), biotite (0.01%), garnet (0.01%), ilmenite (0.02%), and titanite (0.20%). Piccos Brook Member sandstone yields 562 ± 10 Ma to 699 ± 19 Ma detrital zircon grains with age maxima of 618 Ma and single-grain ages of 721 ± 19 Ma to 3220 ± 27 Ma (Fig. 9, n = 94/98).

4.5. Blackhead Formation

Maddox Cove and Spriggs Point Member samples (02LB15, 03LB15 in Fig. 4D) have 45.27% and 45.08% quartz, respectively, but the latter has 3 times more (6.29%) potassium feldspar (Table S1). Maddox Cove Member sandstone yields the highest biotite (0.05%) and ilmenite (0.05%) abundances in the sample suite, and 0.08% allanite, 0.05% apatite, 0.01% garnet, and 0.73% titanite. Sample 02LB15 mostly yields 566 ± 8 Ma to 700 ± 9 Ma detrital zircon grains with age maxima of 620 Ma (Fig. 9, n = 97/108). The sample includes single-grain ages of 534 ± 7 Ma to 2109 ± 30 Ma. Detrital zircon grains that comprise the 620 Ma age maxima yield εHf$_{(t)}$ values of +9.8 to −7.6 ($\overline{X}$= +4.3) and three 761–891 Ma detrital zircon grains have εHf$_{(t)}$ values of −6.2 to −20.0 (Fig. 9). Calymmian, Orosirian, and Rhyacian grains have εHf$_{(t)}$ values of +5.6, −1.4, and +4.8, respectively. Spriggs Point Member sandstone has 0.08% allanite, 0.04% apatite, 0.02% biotite, 0.03% ilmenite, and 0.83% titanite (Table S1). Sample 03LB15 mostly yields 567 ± 8 Ma to 716 ± 24 Ma detrital zircons with age maxima of 611 Ma (Fig. 9, n = 100/115). The sample includes 756 ± 11 Ma to 818 ± 14 Ma, 1064 ± 2 Ma to 1100 ± 50 Ma, and 1536 ± 18 Ma to 2060 ± 14 Ma single grains and age fractions. Detrital zircon grains from the 611 Ma age maxima have εHf$_{(t)}$ values of +9.9 to −15.6 ($\overline{X}$= +5.1) whereas 818–756 Ma grains yield εHf$_{(t)}$ values of −4.8 to −16.0 ($\overline{X}$ = −11.6). Meso- to Paleoproterozoic single grains have εHf$_{(t)}$ values of +6.9 to −1.0.

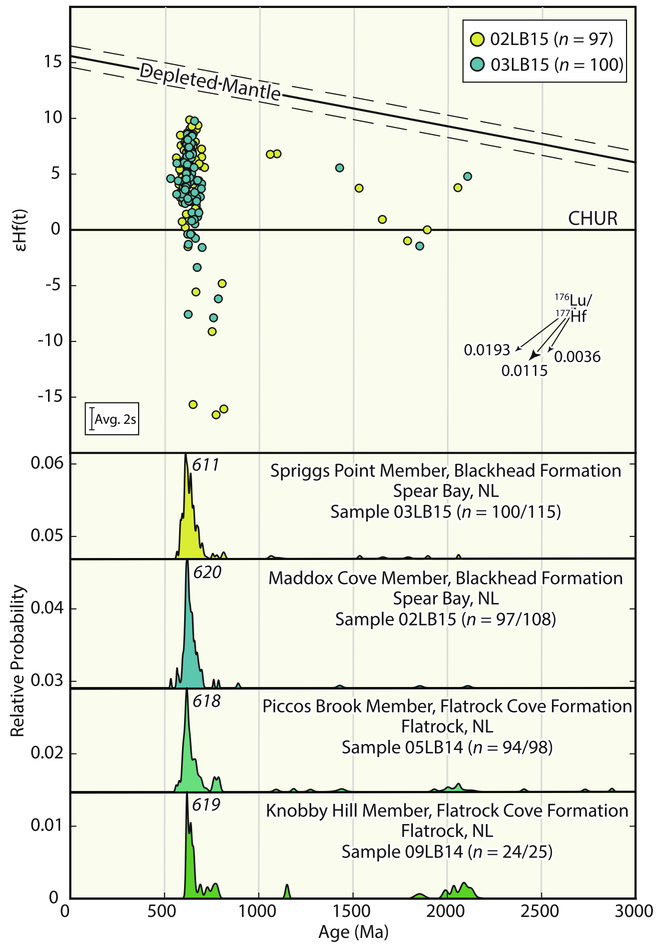

Fig. 9. Detrital zircon results from upper Signal Hill Group rock units: Knobby Hill Member sandstone, Flatrock Cove Formation (09LB14), Piccos Brook Member sandstone, Flatrock Cove Formation (05LB14), Maddox Cove Member sandstone, Blackhead Formation (02LB15), and Spriggs Point Member sandstone, Blackhead Formation (03LB15). CHUR is chondritic uniform reservoir. Crustal evolution trends show an average $^{176}Lu/^{177}Hf$ value of 0.0115 and a range of $^{176}Lu/^{177}Hf$ values of 0.0193 to 0.0036 (e.g., Vervoort et al., 1999). NL - Newfoundland and Labrador. n = number of grains that passed discordance filter against total number of analyses.

5. Discussion

5.1. MDA estimates for Conception and Signal Hill Group strata

Table 1 reports maximum depositional age (MDA) estimates using the YSG, YSP, YGC2σ, and MLA methods. The use of such MDA methods remains a subject of debate (Coutts et al., 2019; Copeland, 2020; Sharman and Malkowski, 2020; Vermeesch, 2021). Although all MDA evaluations must account for real-world complications such as Pb loss, Vermeesch (2021) argued that statistical approaches like the MLA algorithm provide unique MDA values instead of those calculated with ad hoc methods like YSG, YSP, and YGC2σ. The MLA algorithm is set up to converge to the true solution with increasing sample size and uses all sample data (Vermeesch, 2021). Most MDA estimates for each sample overlap within uncertainty, but the YSG method typically gives the youngest values and YSP and YGC2σ methods give the oldest values (Table 1). We preferred the MLA algorithm results when there was disagreement between methods.

5.1.1. Conception Group

Late Ediacaran depositional ages for Conception Group rocks in the St. John's area were originally based on stratigraphic correlations with fossil-bearing rocks in the SE Avalon Peninsula (Williams and King, 1979; King, 1990). Zircon U-Pb studies have subsequently constrained the ages of Conception Group rocks in the SE Avalon Peninsula to between 580 and 565 Ma, including constraints for the lower and upper Drook Formation of 579.88 ± 0.44 Ma and 570.94 ± 0.38 Ma, respectively (Pu et al., 2016; Matthews et al., 2021). Gaskiers Formation diamictites and equivalent rocks in eastern Newfoundland yield zircon U-Pb dates of 579.63 ± 0.15 Ma to 579.24 ± 0.17 Ma (Pu et al., 2016) and overlap with the oldest dated parts of the Drook Formation.

Most MDA estimates for the Torbay and Bauline Line Member samples range from 588 ± 6 Ma to 581 ± 5 Ma and 577 ± 5 Ma to 575 ± 5 Ma, respectively (Table 1). The MLA value for the Torbay Member (588 ± 6 Ma) does not overlap the weighted mean $^{206}Pb/^{238}U$ age of 579.88 ± 0.44 Ma for the lower Drook Formation in the SE Avalon Peninsula (Pu et al., 2016). A potential explanation is that the Torbay Member sample was derived from older arc infrastructure and lacks evidence for syn-depositional, ca. 580 Ma volcanism. Bauline Line Member MDA values overlap the weighted mean $^{206}Pb/^{238}U$ ages for Drook and Gaskiers Formation rocks within uncertainty.

5.1.2. Lower Signal Hill Group

The age of lower Signal Hill Group is generally constrained by 564.71 ± 0.88 Ma and 564.13 ± 0.65 Ma tuffs in the underlying Trepassey and Fermeuse Formations (Matthews et al., 2021). Most MDA estimates for the two Quidi Vidi Formation samples are 582 ± 2 Ma to 582 ± 3 Ma (04LB15) and 613 ± 3 Ma to 604 ± 3 Ma (11LB14), respectively (Table 1). These estimates are older than the ca. 564 Ma tuffs that underlie the Signal Hill Group and indicate that the samples lack evidence for syn-Quidi Vidi Formation volcanism. The MDA estimates instead demonstrate that Quidi Vidi Formation detrital zircon grains have provenance from older arc successions, including ca. 582 Ma Horse Cove complex rocks near Bauline ~10 km to the west and ca. 614–606 Ma rocks of the Harbour Main Group near Conception Bay ~30 km to the southwest (Mills et al., 2021). Cape Spear (13LB14, 14LB14) and Skerries Bight Member (01LB15) samples yield MLA estimations of 589 ± 5 Ma to 562 ± 7 Ma (Table 1) and similarly indicate provenance from adjacent arc rocks and lack of syn-Cuckold Formation volcanism. The abundance of felsic intrusive and volcanic rock fragments in enclosing conglomerate units (Table S4) supports the arc source hypothesis.

Cape Spear Member quartzite clasts yield MLA estimates of 1846 ± 9 Ma (17CP01), 1560 ± 39 Ma (59LB14), 1128 ± 20 Ma (58LB14), and 1123 ± 21 Ma (17CP03). These MDA calculations did not include single-grain analyses in samples 59LB14 (606 ± 12 Ma, 711 ± 8 Ma) and 17CP03 (608 ± 13 Ma) that we interpret as too young for the dataset. CL grain textures suggest that these concordant grains may have been reset or disturbed by metamorphism (Figure S2). For example, the 606 Ma grain spot in 59LB14 is in a CL bright, low U rim, whereas the 711 Ma grain has banded, sector zoning with fir tree-like textures (e.g., Corfu et al., 2003). The 608 Ma grain spot in sample 17CP03 is in the rim zone and adjacent to an older core zone. The ages of these three grains are also typical of Signal Hill Group rocks and a second option is that they are contaminants, most likely as sand grains that filled cracks in the quartzite clasts (see Fig. 5E, 5G).

5.1.3. Upper Signal Hill Group

Knobby Hill and Piccos Brook Member samples mostly yield MDA estimates of 621 ± 5 Ma to 621 ± 4 Ma and 578 ± 8 Ma to 562 ± 12 Ma, respectively (Table 1). These Flatrock Cove Formation samples were collected from the footwall of the Flat Rock thrust and have provenance from the Harbour Main and Conception Groups to the west (King, 1990). The MLA value of the Piccos Brook Member, which overlies Drook Formation rocks in the hanging-wall of the Flat Rock thrust at Red Head, constrains the timing of Avalonian deformation as 562 ± 12 Ma.

Blackhead Formation samples yield MDA estimates that vary by method and include values that do not overlap within uncertainty (Table 1). Maddox Cove (02LB15) and Spriggs Point (03LB15) Member

Table 1
Location and maximum depositional age estimates for Conception and Signal Hill Group strata. MLA - Maximum Likelihood Age of Vermeesch (2021), YGC2σ - Youngest Grain Cluster of Dickinson and Gehrels (2003), YSG - Youngest Single Grain, YSP - Youngest Statistical Population of Coutts et al. (2019). Conc. – concordant, n = number of grains used (only reported for YSP and YGC), MSWD – mean square weighted deviates.

Rock sample	Sub-unit	Latitude (°N)	Longitude (°W)	Field Location	YSG	YSP	YGC2σ	MLA
Signal Hill Group								
Blackhead Formation								
03LB15	Spriggs Point Member	47.5241	−52.6359	Cape Bay	567 ± 8 Ma, 98 % conc.	586 ± 3 Ma, n = 7, MSWD = 1.1	583 ± 4 Ma, n = 3	570 ± 9 Ma
02LB15	Maddox Cove Member	47.5214	−52.6331	Cape Bay	534 ± 7 Ma, 99 % conc.	566 ± 4 Ma, n = 2, MSWD = 0.0	568 ± 4 Ma, n = 3	538 ± 8 Ma
Flatrock Cove Formation								
05LB14	Piccos Brook Member	47.7054	−52.7100	Flatrock	562 ± 10 Ma, 95 % conc.	578 ± 8 Ma, n = 2, MSWD = 0.1	571 ± 6 Ma, n = 3	562 ± 12 Ma
09LB14	Knobby Hill Member	47.6993	−52.6996	Flatrock	617 ± 8 Ma, 97 % conc.	621 ± 4 Ma, n = 6, MSWD = 0.9	621 ± 4 Ma, n = 6	621 ± 5 Ma
Cuckold Formation								
01LB15	Skerries Bight Member	47.5238	−52.6248	Cape Bay	575 ± 7 Ma, 102 % conc.	602 ± 2 Ma, n = 15, MSWD = 1.0	604 ± 2 Ma, n = 19	589 ± 5 Ma
58LB14	Quartzite clast, Cape Spear Member	47.6973	−52.7105	Flatrock	1115 ± 17 Ma, 99 % conc.	1136 ± 8 Ma, n = 2, MSWD = 0.1	1132 ± 7 Ma, n = 3	1128 ± 20 Ma
59LB14	Quartzite clast, Cape Spear Member	47.6973	−52.7105	Flatrock	1032 ± 9 Ma, 99 % conc.	1563 ± 13 Ma, n = 3, MSWD = 1.0	1572 ± 11 Ma, n = 6	1560 ± 39 Ma
17CP03	Quartzite clast, Cape Spear Member	47.6646	−52.6701	Torbay Point	1121 ± 16 Ma, 98 % conc.	1373 ± 19 Ma, n = 4, MSWD = 1.4	1383 ± 16 Ma, n = 5	1123 ± 21 Ma
17CP01	Quartzite clast, Cape Spear Member	47.6646	−52.6701	Torbay Point	1837 ± 29 Ma, 99 % conc.	1846 ± 7 Ma, n = 4, MSWD = 0.3	1851 ± 6 Ma, n = 5	1846 ± 9 Ma
13LB14	Cape Spear Member	47.6973	−52.7105	Flatrock	565 ± 11 Ma, 100 % conc.	569 ± 8 Ma, n = 14, MSWD = 1.1	575 ± 4 Ma, n = 6	569 ± 7 Ma
14LB14	Cape Spear Member	47.6973	−52.7105	Flatrock	560 ± 8 Ma, 100 % conc.	577 ± 3 Ma, n = 8, MSWD = 0.7	568 ± 4 Ma, n = 4	562 ± 7 Ma
Quidi Vidi Formation								
04LB15		47.6879	−52.7081	Flatrock	570 ± 14 Ma, 90 % conc.	582 ± 2 Ma, n = 12, MSWD = 0.9	582 ± 3 Ma, n = 7	582 ± 3 Ma
11LB14		47.6915	−52.7103	Flatrock	596 ± 10 Ma, 94 % conc.	604 ± 3 Ma, n = 14, MSWD = 1.2	606 ± 2 Ma, n = 22	613 ± 3 Ma
Conception Group								
Drook Formation								
08LB14	Bauline Line Member	47.7025	−52.7139	Flatrock	562 ± 12 Ma, 97 % conc.	577 ± 5 Ma, n = 4, MSWD = 1.1	575 ± 4 Ma, n = 5	575 ± 5 Ma
03LB14	Torbay Member	47.7073	−52.7093	Flatrock	572 ± 8 Ma, 90 % conc.	588 ± 5 Ma, n = 3, MSWD = 1.2	581 ± 5 Ma, n = 3	588 ± 6 Ma

samples have YSP and YGC2σ values that are 10–20 Myr older than those calculated by YSG and MLA methods. One explanation is that the MLA estimate aligns with the YSG value because the difference between the youngest and second youngest grains in these two samples is greater than their analytical uncertainties (Vermeesch, 2021). We prefer MLA estimates for the Maddox Cove and Spriggs Point Members of 538 ± 8 Ma and 570 ± 9 Ma, respectively (Table 1).

5.2. *Evaluating the cratonic affinities of Signal Hill Group quartzite clasts*

Cape Spear Member quartzite clasts yield MDA estimates and mineral compositions that are consistent with their origins as passive margin rocks. Quartzites are also recognized in the oldest West Avalonia successions of Nova Scotia and New England and may overlie Paleo- to Mesoproterozoic crust (e.g., Barr et al., 2003; Thompson et al., 2012; Henderson et al., 2016). The Cape Spear Member quartzite clasts and 54 detrital zircon grains in Signal Hill Group strata that range from 1064 to 3220 Ma occur in fluvial units with igneous rock clasts and were deposited during the unroofing of arc complexes (King, 1990). The quartzite clasts may therefore comprise sub-arc basement rocks exhumed during Avalonian deformation. Evidence for 1378 Ma inherited zircon in the Horse Cove complex (Skipton et al., 2013) and the Nd-Hf isotope compositions of some Avalonian igneous rocks (e.g., Pollock et al., 2019) are consistent with Mesoproterozoic or older sub-arc basement. It is also feasible that the clasts and 1064–3220 Ma detrital zircon grains were derived from an adjacent crustal block that interacted with, but does not underlie, West Avalonia.

Fig. 10A and 10B are MDS plots that use the Kolmogorov-Smirnov (K-S) D-statistic to display differences between the U-Pb and U-Pb-Hf isotope signatures, respectively, of Cape Spear Member quartzite clasts and West African, Amazonian, Ganderian, and Baltican rock units. Although K-S dissimilarities are sensitive to sample size, Vermeesch (2018) concluded that corresponding MDS plots provide sensible configurations, especially as most detrital studies rely on the relative differences between age distributions. Sundell and Saylor (2021) further argued that the K-S D-statistic shows lower sensitivity to sample size effects than other methods. Detrital zircon studies have effectively used the K-S D-statistic to resolve provenance trends, including datasets with differences in sample size (Gehrels et al., 2020; McClelland et al., 2021, 2023).

5.2.1. *West Africa*

The West African craton is typically dismissed as a source for West Avalonia rocks (e.g., Murphy et al., 2004; Henderson et al., 2016), in part because of the ca. 1700–1000 Ma magmatic gap in the Leo-Man and Reguibat shields and abundance of carbonate strata in Taoudeni basin cover assemblages that are rare in Avalonia (Bradley et al., 2022). However, recent plate tectonic reconstructions have proposed that Avalonia was proximal to the West African craton during the Meso-proterozoic to Neoproterozoic (Fig. 11A; see Evans, 2021) and could

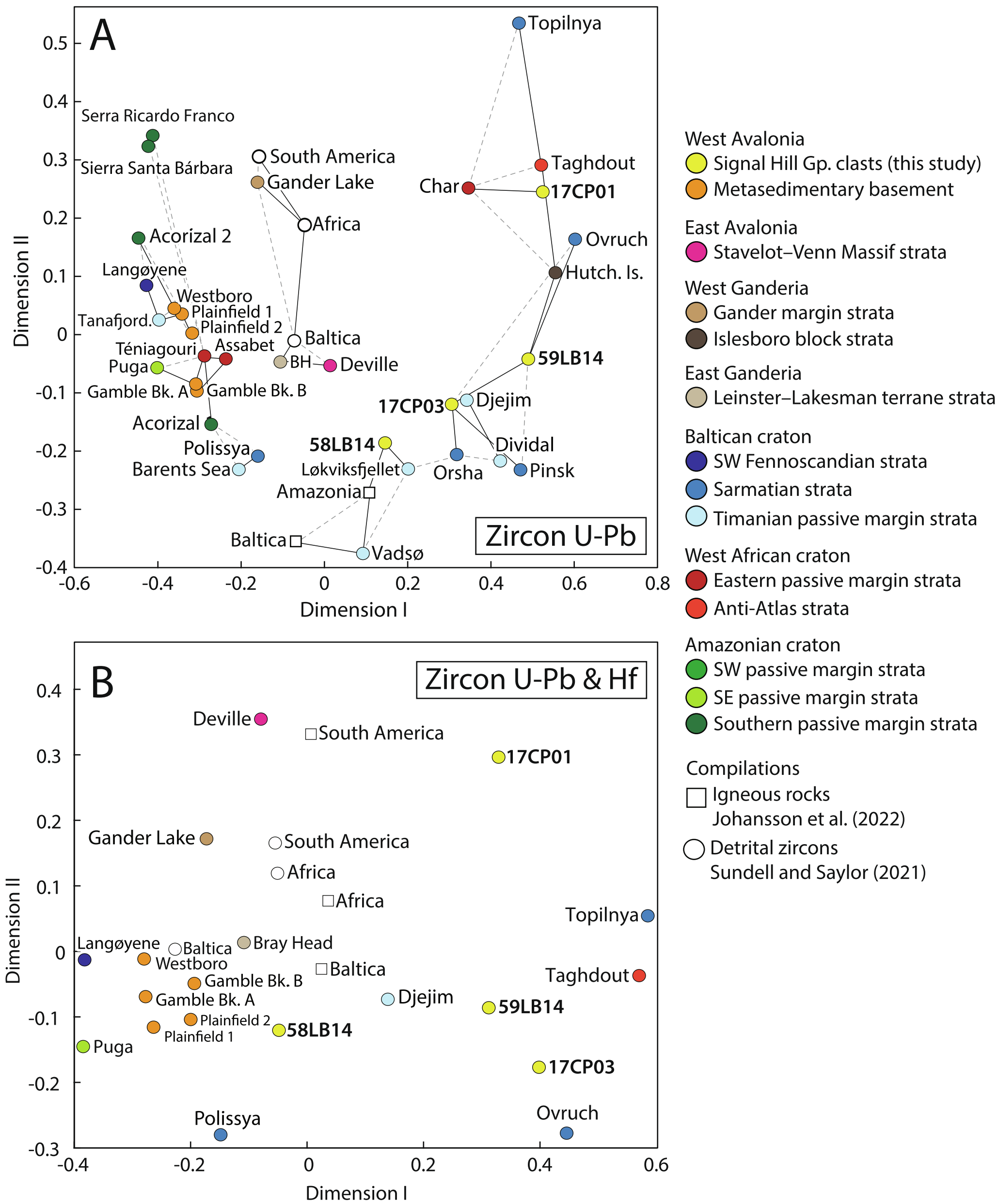

Fig. 10. 2D multidimensional scaling plots of (A) detrital zircon U–Pb age signatures and (B) detrital zircon U-Pb-Hf isotope signatures of four Cape Spear Member quartzite clasts (58LB14, 59LB14, 17CP01, 17CP03) and global reference frames using the K-S D-statistic (see text for information). Solid black lines and dotted gray lines in Fig. 10A are closest and second-closest statistical neighbors, respectively. West Avalonia: (Signal Hill Group clasts - this study; Gamble Brook Formation - Henderson et al., 2016; Plainfield and Westboro Formations - Severson et al., 2016). East Avalonia: Stavelot-Venn Massif (Deville Formation - Willner et al., 2013). West Ganderia: Gander margin (Gander Lake Group - Willner et al., 2014); Islesboro block (Hutchins Island Quartzite - Reusch et al., 2018). East Ganderia: Leinster-Lakesman terrane (Bray Head Formation - Waldron et al., 2019). Baltica: Fennoscandian craton (Langøyene Formation - Kristoffersen et al., 2014); Sarmatian craton (Polissya, Ovruch, and Topilnya Series - Shumlyanskyy et al., 2015; Pinsk and Orsha Series - Paszkowski et al., 2019); Timanian passive margin (Djejim Formation, Kuznetsov et al., 2010; Dividal, Løkviksfjellet, Tanafjorden, Vadsø Groups - Zhang et al., 2015). West African craton (Char, Assabet, and Teniagouri barcodes - Bradley et al., 2022; Taghdout Group - Abati et al., 2010, 2012). Amazonian craton (SW passive margin, Aguapeí Group, Serra Ricardo Franco, and Sierra Santa Bárbara units - Geraldes et al., 2014; SE passive margin, Alto Paraguay Group, Puga Formation - McGee et al., 2015; southern passive margin, Cuiabá Group, Acorizal Formation - Babinski et al., 2018).

have ties with Taoudeni basin rocks. Bradley et al. (2022) defined detrital zircon barcodes for Taoudeni basin units in Mauritania, including the ca. 1100 Ma Char Group and ca. 883–570 Ma Assabet el Hassiane Group. Whereas the Char barcode is diagnostic of underlying rocks and yields 2941, 2871, 2703, 2447, 2076, and 2041 Ma age maxima, the Assabet barcode has 1510, 1212, 1021, and 936 Ma age maxima that have no known sources in West Africa (Bradley et al., 2022). Bradley et al. (2022) proposed that the Assabet barcode records a Tonian to Cryogenian fluvial system which delivered Amazonian sediment to the West African craton and perhaps the periphery of Baltica (Fig. 11A).

Char and Taghdout (Abati et al., 2012) Group strata that unconformably overlie Paleoproterozoic crystalline rocks cluster in U-Pb MDS space and are close neighbours of 17CP01 (Fig. 10A). Although Wissink et al. (2018) concluded that MDS comparisons are influenced by differences in small (~5%) populations, the Char barcode has 18% Neoproterozoic grains (inferred as spurious by Bradley et al., 2022) that are absent in 17CP01 and Taghdout Group strata, but did not affect their statistical correlations. Paleoproterozoic (ca. 2000 Ma) Topilnya Series strata that overlie Sarmatian basement in the Ukrainian Shield (Shumlyanskyy et al., 2015) are also neighbours of 17CP01 and Char and Taghdout Group rocks (Fig. 10A), which demonstrate the shared tectonomagmatic histories of West Africa and Baltica. Detrital zircon Hf isotope data for the Char barcode are not available, but 17CP01 is different from the Taghdout Group in U-Pb-Hf MDS space and plots closer to Topilnya Series rocks and South American reference frames (Fig. 10B).

Cape Spear Member quartzites are statistically dissimilar to the Assabet barcode and the younger, ca. 569 Ma Téniagouri barcode (Fig. 10A) defined by Bradley et al. (2022) and therefore connections with the West African craton are unlikely. West African reference frames cluster together in the U-Pb MDS plot and are close neighbours of Neoproterozoic passive strata of SE Amazonia (Puga Formation, McGee et al., 2015) and West Avalonia rocks in Nova Scotia (Gamble Brook Formation, Henderson et al., 2016) and New England (Westboro and Plainfield Formations, Severson et al., 2022). Future detrital zircon Hf data are required to test the hypothesis of Bradley et al. (2022), but the available results are consistent with Tonian to Cryogenian fluvial system

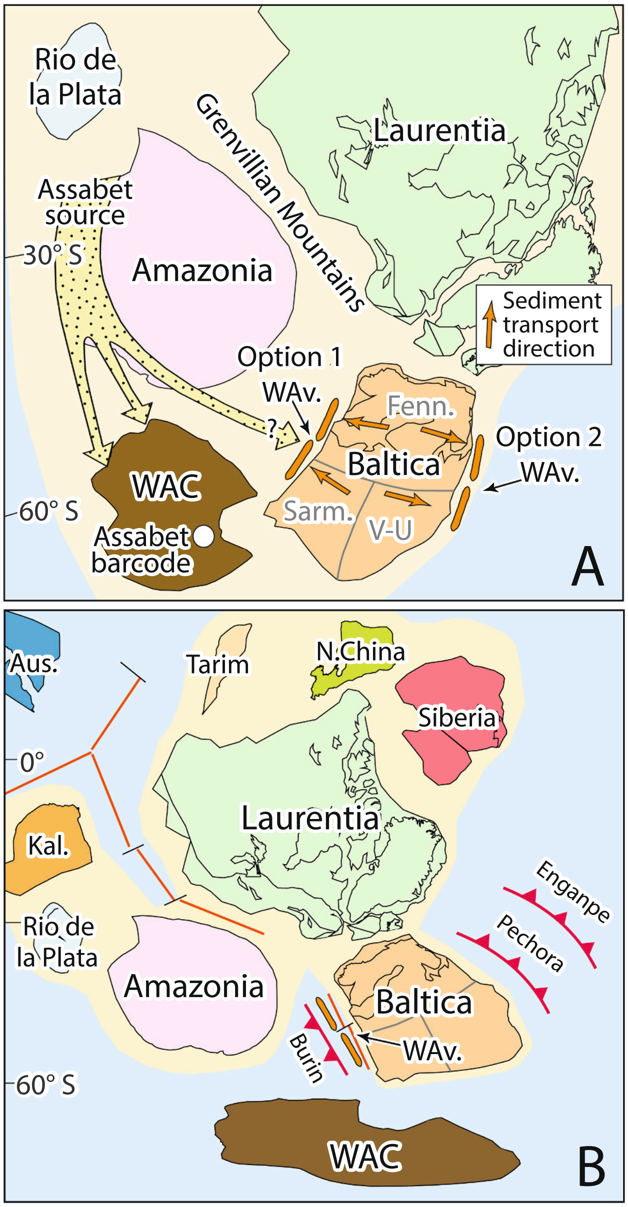

Fig. 11. Cartoon paleogeographic maps of proto-West Avalonia (WAv.) with respect to the Amazonian, Baltican, West African, and adjacent cratons modified from Evans (2001) and Bradley et al. (2022). (A) ca. 900 Ma reconstruction with proto-West Avalonia basement units in Newfoundland and New England-Nova Scotia having origins near Sarmatia and southern Fennoscandia (Option 1, e.g., van Staal et al., 2021a) or Timanian passive margin near northern Fennoscandia and Volgo-Uralia (Option 2, e.g., Landing et al., 2022). Orange arrows indicate expected sediment transport directions. The Assabet barcode in West African craton implies continental drainage system with headwaters in Amazonia (Bradley et al., 2022). (B) ca. 760 Ma reconstruction with preferred southern Baltican origin for West Avalonia basement rocks in Canadian Appalachians. Tonian rifting separated proto-Avalonia sliver(s) from southern Baltica within the nascent Tornquist Ocean (see Evans, 2021). Burin arc interacts with proto-Avalonia sliver ~760 Ma. Pechora and Enganpe arc systems in the pre-Uralian Ocean are schematically shown offshore of the Timanian passive margin (after Pease, 2021). Aus. - Australian cratons, Fenn - Fennoscandia, Kal. - Kalahari, Sarm. - Sarmatia, V-U - Volgo-Uralia, WAC - West African craton. (For interpretation of the references to colour in this figure legend, the reader is referred to the web version of this article.)

that transferred sediment from Amazonia to the West African craton.

5.2.2. Amazonia

Avalonia is generally known as a peri-Gondwanan terrane because of its oft-proposed location along West Gondwana during the Cryogenian to Cambrian (e.g., Murphy et al., 2023). Tectonic models for Avalonia that corroborate this position include a 665–650 Ma arc-continent collision with Amazonia followed by the establishment of an Ediacaran arc (e.g., Nance et al., 2008). Avalonian arc fragments could have been imbricated with Cryogenian and older passive margin successions of Amazonia during arc-collision and resulted in West Avalonia basins receiving detritus from the Rondonian-San Ignácio (1590–1300 Ma), central Amazonian (>2500, 1820–1600 Ma), and Trans-Amazonian (2260–1950 Ma) provinces (e.g., Pollock et al., 2009; Willner et al., 2013). Although the Amazonian and Baltican cratons have shared Proterozoic tectonomagmatic histories, which may result in non-unique provenance interpretations, Amazonian igneous rocks have 2190, 2145, and 2095 Ma (Trans-Amazonian orogen), 1430 Ma (Santa Helena-Alto Guaporé arc), and 1340 Ma (Paraguá accretion) age maxima that are less typical of Baltica (Johansson et al., 2022). Cape Spear Member quartzite clasts do not yield such age maxima and show statistical dissimilarities with Neoproterozoic strata derived from the Amazonian craton. For example, rock units of the southwestern (Aguapeí Group, Geraldes et al., 2014), southeastern (Puga Formation, McGee et al., 2015), and southern (Acorizal Formation, Babinski et al., 2018) passive margins of Amazonia have ca. 1340–1450 Ma, 970–1000 Ma and 1560 Ma, and 1200–1250 and 1550 Ma age maxima, respectively, and plot on the left side of the U-Pb MDS map, indicating dissimilarities with Cape Spear Member samples, some Timanian passive margin of NE Baltica (e.g., Zhang et al., 2015), and Sarmatian craton strata (Fig. 10A). These Amazonian samples instead mostly plot near Gamble Brook, Westboro, and Plainfield Formation rocks, Assabet barcode, and Paleozoic strata of the Oslo rift (Langøyene Formation, Kristofferson et al., 2014) in SW Baltica. Statistical comparisons are hampered by limited detrital zircon Hf isotope data for Amazonian passive margin rocks, but only 58LB14 plots near Puga Formation strata, and is more broadly part of a cluster in Fig. 10B that includes West Avalonia rocks in New England and Nova Scotia and the Baltican detrital zircon reference frame (Sundell and Saylor, 2021). Cape Spear Member clasts are unlikely to have Amazonian provenance, either as eroded fragments of quartzite basement that underpin the Avalon Peninsula or cratonal or passive margin sources after West Avalonia arc-collision.

5.2.3. Ganderia

Ganderia is a large superterrane exposed in the southern Caledonides and core of the northern Appalachian orogen (Fig. 1A, e.g., van Staal et al., 1998; Waldron et al., 2019). Ganderian terranes in the Appalachians are underlain by undated platformal siliciclastic and carbonate successions that were intruded and covered by ca. 650–535 Ma arc rocks (e.g., van Staal et al., 2021b). van Staal et al. (2021a) recently speculated that 575–550 Ma Avalonian deformation resulted from diachronous, oblique convergence between the West Avalonia and Ganderian arcs along the Amazonian margin. Ganderian platformal successions in the Islesboro and Grand Manan terranes of Maine and New Brunswick occupied the collisional upper plate and are proposed sources for quartzite clasts and metamorphic detritus in West Avalonian basins (van Staal et al., 2021a).

Detrital zircon U-Pb statistical comparisons indicate that samples 17CP01 and 59LB14 are neighbors of the Hutchins Island Quartzite in the Islesboro block of Maine (Fig. 10A, Reusch et al., 2018), which similarly yields 1800–2000 Ma and 2700 Ma age fractions. As described previously, 17CP01 is not statistically different from West African and Sarmatian craton strata that overlie Paleoproterozoic basement (Fig. 10A). Paleoproterozoic (ca. 1750 Ma) strata of the Ovruch Series that sit unconformably on Ukrainian Shield granite (Shumlyanskyy et al., 2015) are also close neighbours of the Hutchins Island Quartzite

(Fig. 10A). The results indicate that such cover assemblages provide non-unique solutions for determining Baltican or West African provenance. Lower Paleozoic strata of the Gander margin (Gander Lake Group, Willner et al., 2014) are statistically dissimilar to the Cape Spear Member clasts and Hutchins Island Quartzite, and instead cluster in U-Pb and U-Pb-Hf MDS space with South American and African detrital zircon reference frames (Fig. 10A, 10B). Bray Head Formation strata of East Ganderia (Leinster-Lakesman terrane; Waldron et al., 2019) also show U-Pb and U-Pb-Hf statistical similarities with the Baltican detrital zircon reference frame, Assabet barcode, and West Avalonian quartzites in Nova Scotia and New England (Fig. 10A, 10B). We conclude that the Cape Spear Member clasts were not sourced from Ganderia based the published data, but future studies of Ediacaran basins and Cambrian-Ordovician overstep assemblages are warranted to test this hypothesis.

5.2.4. Baltica

There is growing consensus for West Avalonia rocks in the U.S. and Canadian Appalachians to represent pieces of Baltican crust or have provenance ties with the Baltican craton (Thompson et al., 2012; Henderson et al., 2016; Kuiper et al., 2022; Severson et al., 2022). For example, Gamble Brook Formation quartzites in Nova Scotia yield ca. 1000, 1200, 1500, and 2000 Ma detrital zircon age maxima and Hf isotope compositions that indicate a paleogeographic position near the Telemarkia province, Trans-Scandinavian belt, and Osnitsk-Mikashevychi belt of southern Fennoscandia and western Sarmatia (Henderson et al., 2016). These detrital zircon results and paleomagnetic (e.g., Keppie and Keppie, 2014) interpretations have informed recent plate tectonic models for West Avalonia, although there is debate about its position near SW Baltica (Option 1 in Fig. 11A, van Staal et al., 2021a) or NE Baltica (Option 2 in Fig. 11A, Landing et al., 2022).

Cape Spear Member samples 58LB14, 17CP03, and 59LB14 are close statistical neighbours in U-Pb MDS space (Fig. 10A) with Cryogenian to Ediacaran strata of the Timanian passive margin in the NW Russia and NE Norway sectors of northern Fennoscandia (Djejim Formation, Kuznetsov et al., 2010; Dividal and Løkviksfjellet Groups, Zhang et al., 2015) and ca. 1200 Ma cover assemblages of the Sarmatian craton in Belarus (Pinsk and Orsha Series, Paszkowski et al., 2019) characterized by ca. 1500 and 1900–2200 Ma age maxima; samples 17CP01 and 59LB14 plot in U-Pb space near Orosirian to Statherian cratonal rocks in Ukraine (Topilnya and Ovrush Suites, Shumlyanskyy et al., 2015) based on their abundance of >2200 Ma age maxima and age fractions. West Avalonian rocks of Baltican cratonic affinity in New England (Westboro and Plainfield Formations, Severson et al., 2022) and Nova Scotia (Gamble Brook Formation, Henderson et al., 2016) plot in a separate cluster (Fig. 10A) with the Assabet barcode, SE Amazonian (Puga Formation, McGee et al., 2015) and SW Amazonian passive margin strata (Acorizal Formation, Babinski et al., 2018), some Tonian to Cryogenian strata of the Timanian margin (Tanafjorden and Barents Sea Group, Zhang et al., 2015), Stenian strata of Ukraine (Polissya Series, Shumlyanskyy et al., 2015), and Paleozoic Oslo rift strata in southern Norway (Langøyene Formation, Kristofferson et al., 2014) with 1000–1500 Ma age maxima. In the U-Pb-Hf MDS map (Fig. 10B), Cape Spear Member samples 59LB14 and 17CP03 plot near Djejim Formation and Ovruch Suite rocks of the Timanian margin and Sarmatian craton, respectively, whereas 58LB14 is part of a cluster that includes the Gamble Brook, Plainfield, and Westboro Formations. Although Baltica and Amazonia have shared Paleoproterozoic histories (Johansson et al., 2022), Henderson et al. (2016) concluded that ca. 2250–1900 Ma igneous rocks of Amazonia were uniformly mixed with Archean crust and resultant detrital zircon grains lack depleted mantle-like Hf isotope compositions, whereas Baltica underwent juvenile Ryachian magmatism prior to 2050–1900 Ma magmatism and mixing of depleted mantle with older crust. The Cape Spear Member clasts, most prominently 17CP03, yield ca. 2250–1900 detrital zircon grains with juvenile to depleted mantle-like Hf isotope compositions (Fig. 8) and support Baltican sources as per Henderson et al. (2016).

Avalonia is a composite terrane defined by latest Ediacaran to Ordovician overstep assemblages (Keppie, 1985) and therefore its various basement domains may have different provenance. Our working hypothesis is that Gamble Brook, Plainfield, and Westboro Formation rocks in the northern U.S. and mainland Canadian Appalachians mostly have SW Fennoscandian provenance characterized by ca. 1000–1500 Ma detrital zircon age fractions, whereas Cape Spear Member clasts have greater Sarmatian and northern Fennoscandian craton contributions from >1500 Ma rocks that are more typical of Timanian passive margin and Ukrainian Shield strata. Although speculative, these detrital zircon provenance variations may indicate geographic differences in the original sites of deposition or the Fennoscandian- to Sarmatian-dominant affinities of underlying basement (Fig. 11A). On the other hand, Cape Spear Member clasts have MDA estimates of 1846–1123 Ma (Table 1), which are comparable to those proposed for Orosirian to Stenian strata in Ukraine and Belarus (Shumlyanskyy et al., 2015; Paszkowski et al., 2019), but older than West Avalonian rocks in New England (ca. 959–600 Ma; Kuiper et al., 2022; Severson et al., 2022) and Nova Scotia (ca. 970–750 Ma; Henderson et al., 2016; White et al., 2022). It follows that the Avalon Peninsula clasts could be derived from older successions and statistically different from the rock units in the U.S. and mainland Canadian Appalachians. However, Tonian to Ediacaran strata of the Timanian passive margin mostly have ca. 1800–1000 Ma MDA estimates that are much older than the time of deposition, typical of recycling processes in extensional settings (e.g., Zhang et al., 2015).

5.3. Tonian to Ediacaran tectonic evolution of West Avalonia in eastern Newfoundland

The zircon U-Pb ages and geochemical compositions of Neoproterozoic rocks, in combination with evidence for deformation and metamorphism, have constrained the evolution of West Avalonia (Fig. 12A; e.g., Bevier and Barr, 1990; Kerr et al., 1995; Barr and White, 1996; Murphy et al., 1990, 1999, 2008; O'Brien et al., 1996; Pe-Piper and Piper, 1989, Samson et al., 2000; Nance et al., 2002, 2008; Thompson et al., 2012; Pollock et al., 2019, 2022; White et al., 2021, 2022). Here we use the Baltican cratonic affinities of quartzite units and Ediacaran detrital zircon record (Fig. 12B) to further characterize the tectonic evolution and paleogeography of West Avalonia.

5.3.1. Tonian

The rift histories of the Fennoscandian, Sarmatian, and Volgo-Uralian cratons are uncertain, but the breakup of Rodinia may have established Tonian passive margins along the southern (Ukrainian Shield area) and northeastern (Timanian or pre-Uralian) sides of Baltica (e.g., Meert and Torsvik, 2003; Evans, 2021; Salminen et al., 2021). van Staal et al. (2021a) proposed that ca. 800 Ma extension resulted in the generation of a proto-Avalonia sliver in the nascent Tornquist Ocean between Baltica and Amazonia (Fig. 11B), which following the terminology of Peron-Pinvidic and Manatschal (2010) could have been a continental ribbon that was attached to Baltica, a microcontinent flanked on either side by oceanic crust, a thinned and fault-bounded hanging-wall block, or an unrooted extensional allochthon. Inferred microcontinents in the pre-Uralian ocean, which are now in the Timanides of NW Russia (e.g., Boshezemel block, Pease, 2021), have Mesoproterozoic crust and potentially analogous to the rifted proto-Avalonia sliver (Fig. 11B). If the Tornquist Ocean did not open during the Tonian (e.g., Robert et al., 2021), another model for passive margin generation includes the ca. 800 Ma rifting of a continental margin-fringing arc built on Paleo- to Mesoproterozoic crust (Murphy, 2002; Henderson et al., 2016) and opening of a marginal ocean basin near the Baltica-Amazonia-West Africa nexus.

Tonian rocks that correspond with the ca. 800 Ma rifting event are not recognized in the Avalon Peninsula, however, igneous and pyroclastic units with arc-rift affinities cover and intrude the Gamble Brook Formation and are potential candidates in the Bass River block of Nova

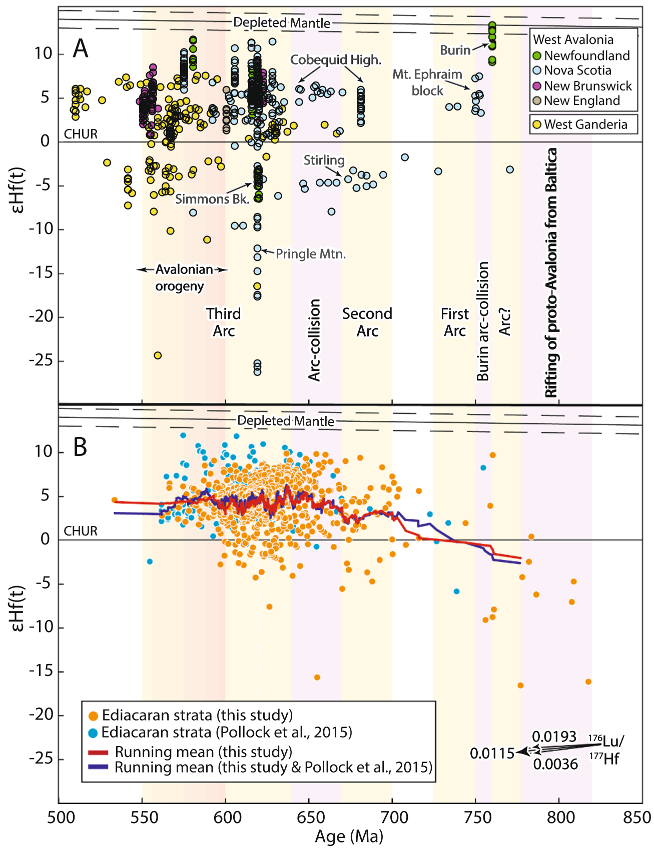

Fig. 12. Tonian to Ediacaran crustal evolution of West Avalonia. (A) εHf(t) vs U-Pb age compilation of representative igneous rocks in the Canadian and northern U.S. Appalachians (Kerr et al., 1995; Pe-Piper and Piper, 1998; Samson et al., 2000; Murphy et al., 2008a, 2008b; Thompson et al., 2012; Skipton et al., 2013; Willner et al., 2013; Pollock et al., 2015, 2022; Henderson et al., 2018; White et al., 2021, 2022 and references therein). Tectonic evolution of West Avalonia adapted from van Staal et al. (2021a). Whole-rock Nd isotope results converted to εHf(t) using the equation of Vervoort and Blichert-Toft (1999). (B) εHf(t) vs U-Pb age summary and running averages of Tonian to Ediacaran detrital zircon grains in Conception and Signal Hill Group strata from this study and Pollock et al. (2015). CHUR is chondritic uniform reservoir. Crustal evolution trends show an average ^{176}Lu/^{177}Hf value of 0.0115 and a range of ^{176}Lu/^{177}Hf values of 0.0193 to 0.0036 (e.g., Vervoort et al., 1999).

Scotia (Pe-Piper and Murphy, 1989; Pe-Piper and Piper, 1989). White et al. (2022) also reported ca. 800–770 Ma detrital and inherited zircon grains in Ephraim block units of Nova Scotia. Ediacaran strata yield 818–775 Ma detrital zircon grains (Fig. 12B) that are potentially derived from such igneous rocks and have subchrondritic $\varepsilon Hf_{(t)}$ values of −16.5 to −2.4 ($\overline{X} = -8.2$), which requires Meso- to Paleoproterozoic depleted mantle ages and contamination of Tonian magmas with evolved crust.

Burin Group rocks represent the vestiges of a juvenile, ca. 765–763 Ma arc system that is interpreted to have interacted with the proto-Avalonian sliver or ribbon arc ~760–750 Ma (Murphy et al., 2008a; van Staal et al., 2021a). The Burin arc phase is archived by an eight-grain population of 766–759 Ma detrital zircons, which includes two 761–760 Ma grains with subchrondritic $\varepsilon Hf_{(t)}$ values of −8.8 and −7.9 and two 760–759 Ma grains with chondritic to superchondritic $\varepsilon Hf_{(t)}$ values of +3.9 and +9.7 (Fig. 12B). Whereas the latter grains are consistent with mantle source regions for Burin Group rocks (Murphy et al., 2008a), those with subchondritic $\varepsilon Hf_{(t)}$ values require an influence from evolved, subducted sediment or that the Burin arc was partially built on Meso- to Paleoproterozoic crust (Henderson et al., 2016). The ~ 760–750 Ma obduction of Burin Group units against the proto-Avalonian sliver or arc ribbon is not recognized in the igneous rock record of eastern Newfoundland, but there are 756 Ma and 755 Ma single-grains in our dataset that yield $\varepsilon Hf_{(t)}$ values of −9.1 and +8.3, respectively (Fig. 12B). Tonian obduction processes may not have occurred along the length of the arc system (van Staal et al., 2021a) and along-strike convergence is possibly recorded by 755–750 Ma arc rocks in Nova Scotia (Fig. 12A; see White et al., 2022). Other options to explain these data include post-collisional subduction initiation, slab window, or slab breakoff processes like those developed for the Taconic cycle along eastern Laurentia (van Staal and Barr, 2012), which included the obduction of the Lushs Bight oceanic tract onto the Dashwoods microcontinent and later growth of the Notre Dame arc and Baie Verte oceanic tract.

The first arc phase for composite West Avalonia (Fig. 12A) was established on the combined Burin terrane-proto-Avalonia sliver/arc ribbon by the late Tonian and is characterized by intermediate to felsic rocks of the 729 ± 2 Ma Hawke Hills tuff in Newfoundland (Israel, 1998) and ca. 739–727 Ma Mount Ephraim and Bass River block units in Nova Scotia (Doig et al., 1993; White et al., 2022). The early arc phase is not well represented in the Avalon Peninsula detrital zircon record, but single-grain analyses of 739, 734, and 727 Ma yield $\varepsilon Hf_{(t)}$ values of −5.8, +2.0, and −0.1, respectively; the 739 Ma grain requires some crustal contributions to the arc system (Fig. 12B).

5.3.2. *Cryogenian*

An unresolved issue of West Avalonia evolution concerns the proposed ca. 730–700 Ma magmatic gap, which van Staal et al. (2021a) interpreted as a temporary shut-off of arc magmatism. Despite the apparent absence of igneous rocks of these ages in eastern Newfoundland, Ediacaran strata of the Avalon Peninsula yield minor populations of 730–700 Ma detrital zircon grains, including 11 with $\varepsilon Hf_{(t)}$ values of −1.6 to +7.3 (Fig. 12B). If these detrital zircon grains reflect arc magmatism in West Avalonia, they may represent younger parts of the first arc phase that began ca. 740 Ma. For example, zircon U-Pb ages of 716 ± 3 Ma and 727 ± 4 Ma were recently reported for felsic rocks in Nova Scotia that are spatially associated with older arc plutons (White et al., 2022). A second option is that these detrital zircon grains have ties with ca. 710 Ma rocks assigned to the Stanner Hanter complex or equivalent units of East Avalonia (Schofield et al., 2010), but it is uncertain if East and West Avalonia were connected at this time (e.g., van Staal et al, 2021a).

The second arc phase of composite West Avalonia generated ca. 700–670 Ma calc-alkaline rocks in the Avalon Peninsula, Cape Breton Island, and New Brunswick (Fig. 12A; e.g., Nance et al., 2008; van Staal et al., 2021a). Corresponding detrital zircon grains have $\varepsilon Hf_{(t)}$ values of −5.5 to +9.4 (Fig. 12B) and early Neo - to Mesoproterozoic depleted mantle ages, which require at least some crustal contributions to arc magmatism. A second, 670–640 Ma arc shut-off episode was proposed by van Staal et al. (2021a), but Ediacaran strata have detrital zircon ages that overlap with this time interval, including those with $\varepsilon Hf_{(t)}$ values of −15.6 to +9.8 (Fig. 12B). Ediacaran sandstone units and felsic rock clasts in the Stirling belt of Cape Breton Island also yield zircon U-Pb ages that are within the 670–640 Ma range (Willner et al., 2013). Broadly coeval magmatism, deformation, and metamorphism are recognized in the Islesboro block in Maine (Stewart et al., 2001) and may suggest the partial assembly of West Ganderia or its early tectonic interactions with West Avalonia. If Avalonia's ties with the Timanide arc system are correct (e.g., Murphy et al., 2004), such tectonism could be related to ca. 670 Ma plate tectonic interactions recorded in the Enganepe ophiolite complex (see Scarrow et al., 2001). Regardless, this Cryogenian episode in West Avalonia has generally been connected to an arc-collision event based on erosion, deformation, and high-grade metamorphism (Nance et al., 2008; van Staal et al., 2021a). In the Avalon Peninsula, ductile deformation and amphibolite-grade metamorphism occurred prior to the pre-630 Ma exhumation of Cryogenian plutons and deposition of Ediacaran cover rocks (O'Brien et al., 1996). Although some models have interpreted that Cryogenian arc-continent collision occurred along the Amazonian margin (Nance et al., 2008; Murphy et al., 2013), others have proposed plate convergence with Baltica or another buoyant element (e.g., Thompson et al., 2012; van Staal et al., 2021a; Murphy et al., 2023). The available paleomagnetic evidence is compatible with a location for West Avalonia near Baltica ~650 Ma (e.g., Keppie and Keppie, 2014).

5.3.3. Ediacaran

5.3.3.1. Implications for paleogeographic models. The third arc phase for composite West Avalonia was established by 640 Ma and intermittent across eastern Newfoundland until 564 Ma (e.g., O'Brien et al., 1996; Matthews et al., 2021; Mills et al., 2021). Punctuated, 560–550 Ma bimodal magmatism also occurred in the Connaigre Peninsula (O'Brien et al., 1995) and Caledonia terrane of New Brunswick (Barr et al., 2020), the latter of which has ca. 550 Ma felsic rocks interpreted as the products of super-eruptions during intra-arc extension or mantle plume activity (Escribano et al., 2023). Several models have proposed that Ediacaran magmatism occurred along the northern margin of Gondwana, with transpressional Avalonian deformation, bimodal magmatism, and arc extension heralding the diachronous collision of a spreading ridge and migration of a triple point (e.g., Murphy and Nance, 1989; Murphy et al. 1999, 2004; Nance et al., 2002, 2008). van Staal et al. (2021a) recently argued that such ridge subduction results in localized forearc deformation only and proposed a model with diachronous, oblique convergence between the Caribbean-style West Avalonia arc and Ganderian continental arc along the Amazonian margin. Our new sediment provenance results are not able to refute the ridge subduction or arc-arc collision hypotheses. Similarly, the models that propose Avalonia originated adjacent to the Timanian orogen, prior to latest Ediacaran separation from NE Baltica by ridge-trench collision (Landing, 1996; Landing et al., 2022), are not fully resolved with our new datasets. The Cape Spear Member quartzite clasts have Baltican cratonic affinities, including provenance ties with Tonian to Ediacaran rocks of the Timanian passive margin as required by such models. However, the Timanides are characterized by late Ediacaran to mid-Cambrian deformation and locally high-grade metamorphism and late Cambrian to Ordovician orogenic collapse (e.g., Roberts and Olovyanishnikov, 2004; Pease and Scott, 2009; Willner et al., 2019) that may be inconsistent with West Avalonia. Recent tectonic syntheses have also reinforced Ediacaran-Cambrian ties between Ganderia, Avalonia, and Amazonian margin (van Staal et al. 2021a, 2021b), which contradicts models for an insular Avalonia microcontinent that was removed from Baltica and Gondwana (e.g., Landing et al., 2022). On the other hand, ca. 550 Ma ash beds and detrital zircon age maxima define the Timanian "fingerprint" in NE Norway and NW Russia (e.g., Zhang et al., 2015), which corresponds to the ages of silicic super-eruptions in West Avalonia (e.g., Escribano et al., 2023). Collett et al. (2022) attempted to reconcile Avalonia's ties with both the Timanides and Gondwanan realm by proposing the Ediacaran to Cambrian clockwise rotation of Baltica towards Amazonia, and subsequent transfer of Timanian arc terranes, including Avalonia, into the Tornquist gap via Caribbean-style (see Waldron et al., 2014) arc migration.

5.3.3.2. Implications for Signal Hill Group deposition. Avalonian orogenesis in the NE Avalon Peninsula resulted in the exhumation of Ediacaran arc rocks (King, 1990) and Signal Hill Group strata are correspondingly dominated by ca. 630–580 Ma detrital zircon grains (Fig. 12B). Signal Hill Group strata typically have gravel-sized felsic rock clasts and yield unimodal age maxima that agree with local sources along the north to northeast-trending Topsail fault to the west (Holyrood horst and Bauline areas in Fig. 2, e.g., Skipton et al., 2013). The Topsail fault has a complex history (Rose, 1952), including several km of vertical offset in post-Cambrian time (Miller, 1983), and may have accommodated regional exhumation during the Avalonian orogeny. The uplift and recycling of Drook Formation and other Conception Group rock units, now exposed in the hanging-walls of the north to northeast-trending Flat Rock thrust and Red Head Cove fault (Fig. 4A), may also have delivered 630–580 Ma detrital zircon grains to Signal Hill Group basins. Signal Hill Group strata contain detrital muscovite and garnet grains that are not recognized in underlying, pre-orogenic rocks of the St. John's and Conception Groups (e.g., Papezik, 1973; Table S1), and we interpret that Avalonian exhumation of sub-arc, metamorphic basement rocks also made quartzite clasts and 1064–3220 Ma single detrital zircon grains available to sediment routing systems. The south to southwest-directed rivers of the Cuckold, Flatrock Cove, and Blackhead Formations probably filled axial drainages that were parallel to the trends of such fault-related highlands. Coalescing alluvial fan systems of the upper Flatrock Cove Formation (King, 1990) were deposited in wedge-top or foredeep depozones and fed by transverse routing systems that drained fault scarps and hinterland areas of high relief.

The age of the Signal Hill Group was previously constrained by ca. 564 Ma tuffs in the underlying St. John's Group (Matthews et al., 2021) and ca. 538–529 Ma quartz arenite units of the Random Formation that conformably overlie Ediacaran red beds in the Bonavista Peninsula (e.g., O'Brien and King, 2004). Signal Hill Group rocks in the NE Avalon Peninsula were mostly sourced from older arc successions and our new data generally provide pre-564 Ma MDA estimates that are too old for these *syn*-orogenic deposits (Table 1). However, Maddox Cove Member (Blackhead Formation) strata of the uppermost Signal Hill Group yield a MDA value of 538 ± 8 Ma (MLA method, Table 1). Tuffaceous facies are locally observed in the Maddox Cove Member succession (King, 1990) and may be repositories of ca. 538 Ma detrital zircon grains. Notably, our Maddox Cove Member sample yields the highest biotite and ilmenite abundances in the suite (Table S1), and these minerals are consistent with tuffaceous origins. The 538 ± 8 Ma MDA value is conspicuously like the 537 ± 3 Ma sericite Ar-Ar age for sheared rocks in the Holyrood horst (Sparkes et al., 2021), which implies that this localized deformation was genetically related to volcanism. Such sources are unknown in Newfoundland, but Barr et al. (2023) reported 531.86 ± 0.34 Ma volcanism in Avalonian successions of Cape Breton Island. Arc rocks with ca. 548–532 Ma ages are also known in the Ganderian terranes (see van Staal et al., 2021a) and could also be primary sources for Maddox Cove Member zircon grains if proximal to West Avalonia at that time. Cambrian to Ordovician quartz arenite units of the Avalonian overstep sequence, some of which are micaceous, yield single-grain ages of 542 ± 19 Ma and 535 ± 13 Ma (Pollock et al., 2009) that overlap with the Maddox Cove Member MDA estimate.

5.3.3.3. Implications for West Avalonia crustal evolution. Third arc phase detrital zircon grains yield a running mean $\varepsilon Hf_{(t)}$ vs U-Pb age curve that generally ranges from +3 to +6, with subpeaks ca. 637, 631, 623, and 616 Ma and subtroughs ca. 641, 634, 627, 619, and 610 Ma (Fig. 12B). Although speculative, the ca. 640–600 Ma data characterize ~6–9 Myr-long cycles between subpeaks and subtroughs that may correspond to intra-arc deformation, crustal reworking, magma replenishment, or other processes. For example, these short-lived events could be related to "tectonic switching" or alternating episodes of contraction and extension in retreating arc systems (Collins, 2002; Murphy et al., 2011). The younger, ca. 600–550 Ma detrital zircon grains lack cyclical $\varepsilon Hf_{(t)}$ features in the running mean curve (Fig. 12B), and it is notable that this time frame overlaps with the onset of bimodal magmatism and strike-slip deformation in West Avalonia, which were diachronous and migrated from New England towards Atlantic Canada (e.g., Nance et al., 2008).

The igneous rock record for the third arc phase shows a negative $\varepsilon Hf_{(t)}$ isotope excursion or isotope pull-down ~620 Ma (Fig. 12A, Pollock et al., 2015, 2022). If the continental arc models for West Avalonia (e.g., Nance et al., 2008) are correct, such a negative $\varepsilon Hf_{(t)}$ isotope excursion could indicate the underthrusting of melt-fertile lower crust during intra-arc and retroarc deformation, which results in the partial melting of lithosphere with only minor contributions from asthenospheric mantle (DeCelles et al., 2009). On the other hand, the isotope pull-down is not ubiquitous across West Avalonia and may instead point to the locations of underlying Baltican cratonic affinity basement that contaminated arc magmas. Oceanic or Caribbean-style arc models for West Avalonia between 640 and 600 Ma (e.g., van Staal et al., 2021a) would probably not foster the types of crustal thickening processes that are typical of continental arc systems but are generally consistent with "tectonic switching" events in extensional arcs.

6. Conclusions

Quartzite clasts collected from Signal Hill Group braided fluvial units record the syn-orogenic exhumation of sub-arc basement rocks in the NE Avalon Peninsula and mostly yield 1220, 1510, and 1900–2200 Ma detrital zircon ages. Detrital zircon statistical assessments support proto-Avalonia having provenance ties with the Fennoscandian and Sarmatian cratons, especially Orosirian to Stenian strata of the Ukrainian Shield and Tonian to Ediacaran strata of the Timanian passive margin. These results strengthen published models for the ca. 800 Ma rifting of a proto-Avalonia sliver or ribbon arc from Baltica, its plate tectonic interactions with the oceanic Burin arc by 750 Ma, and establishment of a first arc phase across the composite terrane ~740–730 Ma. The Hf isotope compositions of Tonian detrital zircon grains indicate some Paleo- to Mesoproterozoic crustal contributions to early arc magmatism. Cryogenian detrital zircon populations are consistent with ca. 700–670 Ma arc activity, however, published models for 670–640 Ma arc shut-off are not supported by the data and instead indicate the timing of collision-related magmatism that was coincident with tectonic interactions with the Baltican or Gondwanan margins or a buoyant block. Ediacaran arc magmatism produced 640–600 Ma detrital zircon grains that include 6 to 9 Myr-long, fluctuating cycles in U-Pb-Hf isotope space and may indicate the frequency of convergent margin processes in West Avalonia. These cycles apparently ceased by 600 Ma, coincident with the onset of bimodal magmatism and Avalonian deformation. Latest Ediacaran and younger deformation in the NE Avalon Peninsula resulted in the deposition of terrestrial deposits that were mostly sourced from exhumed arc assemblages. Fluvial systems axially drained fault-related topography in wedge-top or foredeep depozone settings.

CRediT authorship contribution statement

Luke P. Beranek: Conceptualization, Methodology, Validation, Formal analysis, Investigation, Resources, Data curation, Writing – original draft, Visualization, Supervision, Funding acquisition. **Alexander D. Hutter:** Formal analysis, Data curation, Writing – review & editing. **Stephen Pearcey:** Investigation, Formal analysis, Data curation, Writing – review & editing. **Corey James:** Investigation, Formal analysis, Data curation, Writing – review & editing. **Vanessa Langor:** Investigation, Formal analysis, Data curation, Writing – review & editing. **Calum Pike:** Investigation, Formal analysis, Data curation, Writing – review & editing. **Dylan Goudie:** Investigation, Formal analysis, Data curation, Writing – review & editing. **Lindsay Oldham:** Formal analysis, Data curation, Writing – review & editing.

Declaration of Competing Interest

The authors declare that they have no known competing financial interests or personal relationships that could have appeared to influence the work reported in this paper.

Data availability

The research data are available as Supplementary Materials to the manuscript

Acknowledgements

This article is dedicated to Dr. Tomas J. Calon (1947-2021), an outstanding mentor and colleague that introduced us to the Precambrian geology of the St. John's area. Luke Beranek acknowledges funding support from the Research and Development Corporation of Newfoundland and Labrador (Ignite Research & Development Program). John Hanchar and Core Research Equipment & Instrument Training Network staff members Wanda Aylward, Rebecca Lam, Markus Wälle, and Sarah Jantzi aided laboratory studies at Memorial University of Newfoundland. Cees van Staal gave helpful feedback on this research. Journal reviewers J. Brendan Murphy and Damian Nance provided thoughtful and constructive comments that improved this manuscript.

Appendix A. Supplementary material

Supplementary data to this article can be found online at https://doi.org/10.1016/j.precamres.2023.107046.

References

Abati, J., Aghzer, A.M., Gerdes, A., Ennih, N., 2010. Detrital zircon ages of Neoproterozoic sequences of the Moroccan Anti-Atlas belt. Precambr. Res. 181, 115–128. https://doi.org/10.1016/j.precamres.2010.05.018.

Abati, J., Aghzer, A.M., Gerdes, A., Ennih, N., 2012. Insights on the crustal evolution of the West African craton from Hf isotopes in detrital zircons from the Anti-Atlas belt. Precambr. Res. v. 212–213, 263–274. https://doi.org/10.1016/j.precamres.2012.06.005.

Anderson, M.M., Bruckner, W.D., King, A.F., Maher, J.B., 1975. The late Proterozoic "H. D. Lilly Unconformity" at Red Head, northeastern Avalon Peninsula, Newfoundland. Am. J. Sci. 275, 1012–1027. https://doi.org/10.2475/ajs.275.9.1012.

Anderson, M.M., 1987. Stratigraphy of Cambrian rocks at Bacon Cove, Duffs, and Manuels River, Conception Bay, Avalon Peninsula, eastern Newfoundland. In: Roy, D.C., (Ed.), Centennial Field Guide, Volume 5: Boulder, Colorado, Geological Society of America, Northeastern Section, pp. 475–472. https://doi.org/10.1130/0-8137-5405-4.467.

Babinski, M., McGee, B., do Couto Tokashiki, C., Tassinari, C.C.G., Souza Saes, G., Calvacante Pinho, F.E., 2018. Comparing two arms of an orogenic belt during Gondwana amalgamation: age and provenance of the Cuiaba Group, northern Paraguay belt, Brazil. J. South Am. Earth Sci. 85, 6-42. https://doi.org/10.1016/j.jsames.2018.04.009.

Barr, S.M., White, C.E., 1996. Tectonic setting of Avalonian volcanic and plutonic rocks in the Caledonian Highlands, southern New Brunswick, Canada. Can. J. Earth Sci. 33, 156-168. https://doi.org/10.1139/e96-015.

Barr, S.M., Davis, D.W., Kamo, S., White, C.E., 2003. Significance of U-Pb detrital zircon ages in quartzite from peri-Gondwanan terranes, New Brunswick and Nova Scotia, Canada. Precambr. Res. 126, 123–145. https://doi.org/10.1016/S0301-9268(03)00192-X.

Barr, S.M., Johnson, S.C., Dunning, G.R., White, C.E., Park, A.F., Walle, M., Langille, A., 2020. New Cryogenian, Neoproterozoic, and middle Paleozoic U-Pb zircon ages from the Caledonia terrane, southern New Brunswick, Canada: better constrained but more complex volcanic stratigraphy. Atl. Geol. 56, 163–187. https://doi.org/10.4138/atlgeol.2020.007.

Barr, S.M., White, C.E., Palacios, T., Jensen, S., van Rooyen, D., Crowley, J.L., 2023. The Terreneuvian MacCodrum Brook section, Mira terrane, Cape Breton Island, Nova Scotia, Canada: age constraints from ash layers, organic-walled microfossils, and trace fossils. Can. J. Earth Sci. https://doi.org/10.1139/cjes-2022-0044, in press.

Beranek, L.P., Gee, D.G., Fisher, C.M., 2020. Detrital zircon U-Pb-Hf isotope signatures of Old Red Sandstone strata constrain the Silurian to Devonian paleogeography, tectonics, and crustal evolution of the Svalbard Caledonides. Geol. Soc. Am. Bull. 132, 1987–2003. https://doi.org/10.1130/B35318.1.

Beranek, L.P., Nissen, A., Murphy, S., Grant, D., Goudie, D., Oldham, L., Johns-Buss, E.G., 2022. Late Jurassic syn-rift deposition in the Flemish Pass basin, offshore Newfoundland: Evidence for Tithonian magmatism and Appalachian-Variscan sediment sources from quantitative mineral and detrital zircon U-Pb-Hf isotope studies of Mizzen discovery strata. Mar. Pet. Geol. 146, 105960 https://doi.org/10.1016/j.marpetgeo.2022.105960.

Bevier, M.L., Barr, S.M., 1990. U-Pb age constraints on the stratigraphy and tectonic history of the Avalon terrane. New Brunswick, Canada: J. Geol. 98, 53–63. https://doi.org/10.1086/629374.

Bouvier, A., Vervoort, J.D., Patchett, P.J., 2008. The Lu-Hf and Sm-Nd isotopic composition of CHUR: Constraints from unequilibrated chondrites and implications for the bulk composition of terrestrial planets. Earth Planet. Sci. Lett. 273, 48–57. https://doi.org/10.1016/j.epsl.2008.06.010.

Bradley, D.C., Evans, D.A.D., O'Sullivan, P., Taylor, C.D., Eglington, B.M., 2022. The Assabet barcode: mesoproterozoic detrital zircons in Neoproterozoic strata from

Mauritania. West Africa: Am. J. Sci. 322, 939–992. https://doi.org/10.2475/08.2022.01.
Brubacher, A., 2016. Structural geometry and kinematic evolution of the Flat Rock thrust zone, Flatrock Newfoundland: Memorial University of Newfoundland, unpublished BSc honours thesis, 76 pp.
Calon, T.J., 2005. Late Precambrian sedimentation and related orogenesis of the Avalon Peninsula, eastern Avalon zone, Newfoundland: Field Trip Guidebook, Atlantic Universities Geological Conference Annual Meeting. St. John's, Newfoundland and Labrador, p. 35.
Cohen, K.M., Finney, S.C., Gibbard, P.L., Fan, J.-X., 2013. (updated, 2022/10), The ICS International Chronostratigraphic Chart. Episodes 36, 199–2014. http://www.stratigraphy.org/ICSchart/ChronostratChart2022-10.pdf.
Collett, S., Mazur, S., Schulmann, K., Soejono, I., 2022. Significance of a late Neoproerozoic – early Cambrian active margin in late-stage Rodinian and early Gondwanan reconstructions. Precambr. Res. 383, 106918 https://doi.org/10.1016/j.precamres.2022.106918.
Collins, W.J., 2002. Hot orogens, tectonic switching, and creating of continental crust. Geology 30, 535–538. https://doi.org/10.1130/0091-7613(2002)030<0535:HOTSAC>2.0.CO;2.
Colman-Sadd, S., Hayes, J., Knight, I., and Pereira, C.P.G., 1990. The geology of the Island of Newfoundland, map 90-01: Report of Activities, Government of Newfoundland and Labrador, Department of Mines and Energy, Geological Survey Branch, scale 1:1,000,000.
Copeland, P., 2020. On the use of geochronology of detrital grains in determining the time of deposition of clastic sedimentary strata. Basin Res. 32, 1532–1546. https://doi.org/10.1111/bre.12441.
Corfu, F., Hanchar, J.M., Hoskin, P.W.O., and Kinny, P., 2003. Atlas of zircon textures. In: Hanchar, J.M., Hoskin, P.W.O., (Eds.), Zircon: Washington, D.C., Mineralogical Society of America, Reviews in Mineralogy and Geochemistry 53, pp. 469-500. https://doi.org/10.2113/0530469.
Coutts, D.S., Matthews, W.A., Hubbard, S.M., 2019. Assessment of widely used methods to derive depositional ages from detrital zircon populations. Geosci. Front. 10, 1421–1435. https://doi.org/10.1016/j.gsf.2018.11.002.
Dec, T., Knight, I., O'Brien, S.J., 1989. Sedimentological studies of the Eastport basin: notes on the petrography of the Late Precambrian Connecting Point Group and provenance implications: Current Research. Newfoundland Department of Mines, Geological Survey of Newfoundland, Report 89-I, pp. 63-79.
Dec, T., O'Brien, S.J., Knight, I., 1992. Late Precambrian volcaniclastic deposits of the Avalonian Eastport basin (Newfoundland Appalachians): petrofacies, detrital clinopyroxene geochemistry, and paleotectonic implications. Precambr. Res. 59, 243–262. https://doi.org/10.1016/0301-9268(92)90059-W.
DeCelles, P.G., Ducea, M.N., Kapp, P., Zandt, G., 2009. Cyclicity in Cordilleran orogenic systems. Nat. Geosci. 2, 251–257. https://doi.org/10.1038/ngeo469.
Dickinson, W.R., Gehrels, G.E., 2009. Use of U-Pb ages of detrital zircons to infer maximum depositional ages of strata: a test against a Colorado Plateau Mesozoic database. Earth Planet. Sci. Lett. 288, 115–125. https://doi.org/10.1016/j.epsl.2009.09.013.
Doig, R., Murphy, J.B., Nance, R.D., 1993. Tectonic significance of the late Proterozoic Economy River gneiss, Cobequid Highlands, Avalon composite terrane, Nova Scotia. Can. J. Earth Sci. 30, 474–479. https://doi.org/10.1139/e93-035.
Escribano, A.P., Barr, S.M., Crowley, J.L., 2023. Precise U-Pb zircon dates from silicic super-eruptions during late Ediacaran extension in the Avalonian Caledonia terrane of southern New Brunswick, Canada. Can. J. Earth Sci. in press. https://doi.org/10.1139/cjes-2022-0100.
Evans, D.A.D., 2021. Meso-Neoproterozoic Rodinia supercycle. In: Pesonen, L.J., Salminen, J., Evans, D.A.D., Elming, S.-A., Veikkolaninen, T., (Eds.), Ancient Supercontinents and the Paleogeogeography of Earth. Elsevier, pp. 549–576. https://doi.org/10.1016/B978-0-12-818533-9.00006-0.
Evans, B.W., 2010. Structural analysis of the Knobby Hill anticline in the Flat Rock to Torbay area, eastern Avalon zone, Newfoundland: Memorial University of Newfoundland, unpublished BSc honours thesis, 72 pp.
Fisher, C.M., Vervoort, J.D., DuFrane, S.A., 2014. Accurate Hf isotope determinations of complex zircons using the "laser ablation split stream" method. Geochem. Geophys. Geosyst. 15, 121–139. https://doi.org/10.1002/2013GC004962.
Gehrels, G.E., Giesler, D., Olsen, P., Kent, D., Marsh, A., Parker, W., Rasmussen, C., Mundil, R., Irmis, R., Geismann, J., Lepre, C., 2020. LA-ICPMS U-Pb geochronology of detrital zircon grains from the Coconino, Moenkopi, and Chinle formations in the Petrified Forest National Park (Arizona). Geochronology 2, 257–282. https://doi.org/10.5194/gchron-2-257-2020.
Geraldes, M.C., Nogueira, C., Vargas-Mattos, G., Matos, R., Teixeira, W., Valencia, V., Ruiz, J., 2014. U-Pb detrital zircon ages from the Aguapei Group (Brazil): implications for the geological Evolution of the SW border of the Amazonian craton. Precambr. Res. 244, 306–316. https://doi.org/10.1016/j.precamres.2014.02.001.
Grant, D.C., Goudie, D.J., Voisey, C., Shaffer, M., Sylvester, P., 2018. Discriminating hematite and magnetite via Scanning Electron Microscope-Mineral Liberation Analyzer in the -200 mesh size fration of iron ores. Appl. Earth Sci. 127, 30–37. https://doi.org/10.1080/03717453.2017.1422334.
Henderson, B.J., Collins, W.J., Murphy, J.B., Gutierrez-Alonso, G., Hand, M., 2016. Gondwanan basement terranes of the Variscan-Appalachian orogen: Baltican, Saharan and West Africa hafnium isotopic fingerprints in Avalonia, Iberia and the Armorican terranes. Tectonophysics 681, 278–304. https://doi.org/10.1016/j.tecto.2015.11.020.
Henderson, B.J., Collins, W.J., Murphy, J.B., Hand, M., 2018. A hafnium isotopic record of magmatic arcs and continental growth in the Iapetus Ocean: the contrasting evolution of Ganderia and the peri-Laurentian margin. Gondw. Res. 58, 141–160. https://doi.org/10.1016/j.gr.2018.02.015.
Hibbard, J.P., van Staal, C.R., Rankin, D.W., Williams, H., 2006. Lithotectonic map of the Appalachian orogen, Canada – United States of America. Geological Survey of Canada Map 02096A, 2 sheets, scale 1:1,500,000.
Israel, S.A., 1998. Geochronological, structural, and stratigraphic investigation of a Precambrian unconformity between the Harbour Main Group and Conception Group, east coast Holyrood Bay. Memorial University of Newfoundland, Avalon Peninsula, Newfoundland, p. 78 pp. unpublished BSc honours thesis.
Johansson, A., Bingen, B., Huhma, H., Waight, T., Vestergaard, R., Soesoo, A., Skridlaite, G., Krzeminska, E., Shumlyanskyy, L., Holland, M.E., Holm-Denoma, C., Teixeira, W., Faleiros, F.M., Ribeiro, B.V., Jacobs, J., Wang, C., Thomas, R.J., Macey, P.H., Kirkland, C.L., Hartnady, M.I.H., Englington, B.M., Puetz, S.J., Condie, K.C., 2022. A geochronological review of magmatism along the external margin of Columbia and in the Grenville-age orogens forming the core of Rodinia. Precambr. Res. 371, 106463 https://doi.org/10.1016/j.precamres.2021.106463.
Keppie, J.D., Keppie, D.F., 2014. Ediacaran-middle Paleozoic oceanic voyage of Avalonia from Baltica via Gondwana to Laurentia: paleomagnetic, faunal and geological constraints. Geosci. Canada, 41, 5-18. https://doi.org/10.12789/geocanj.2014.41.039.
Keppie, J.D., Davis, D.W., Krogh, T.E., 1998. U-Pb geochronological constraints on Precambrian stratified units in the Avalon composite terrane of Nova Scotia, Canada: tectonic implications. Can. J. Earth Sci. 35, 222–236. https://doi.org/10.1139/e97-109.
Keppie, J.D., 1985. The Appalachian collage. In: Gee, D.G., Sturt, B.A., (Eds.), The Caledonide Orogen: Scandinavia and Related Areas: Wiley, New York, pp. 1217–1226.
Kerr, A., Jenner, G.A., Fryer, B.J., 1995. Sm-Nd isotopic geochemistry of Precambrian to Paleozoic granitoid suites and the deep-crustal structure of the southeast margin of the Newfoundland Appalachians. Can. J. Earth Sci. 32, 224–245. https://doi.org/10.1139/e95-019.
King, A.F., 1990. Geology of the St. John's area: Geological Survey Branch, Department of Mines and Energy, Government of Newfoundland and Labrador, Report 90-2, 93 pp.
Kristoffersen, M., Andersen, T., Andresen, A., 2014. U-Pb age and Lu-Hf signatures of detrital zircon from Palaeozoic sandstones in the Oslo Rift, Norway. Geol. Mag. 151, 816–829. https://doi.org/10.1017/S0016756813000885.
Krogh, T.E., Strong, D.F., O'Brien, S.J., Papezik, V.S., 1988. Precise U-Pb zircon dates from the Avalon terrane in Newfoundland. Can. J. Earth Sci. 25, 442-453. https://doi.org/10.1139/e88-045.
Kuiper, Y.D., Murray, D.P., Ellison, S., Crowley, J.L., 2022. U-Pb detrital zircon analysis of sedimentary rocks of the southeastern New England Avalon terrane in the U.S. Appalachians: Evidence for a separate crustal block. In: Kuiper, Y.D., Murphy, J.B., Nance, R.D., Strachan, R.A., Thompson, M.D., (Eds.), New Developments in the Appalachian-Variscan Orogen: Boulder, Colorado, Geological Society of America Special Paper 554, p. 93-119. https://doi.org/10.1130/2021.2554(05).
Kuznetsov, N.B., Natapov, L.M., Belousova, E.A., O'Reilly, S.Y., Griffin, W.L., 2010. Geochronological, geochemical, and isotopic study of detrital zircon suites from late Neoproterozoic clastic strata along the NE margin of the East European Craton: implications for plate tectonic models. Gondw. Res. 17, 583–601. https://doi.org/10.1016/j.gr.2009.08.005.
Landing, E., Keppie, J.D., Keppie, D.F., Geyer, G., Westrop, S.R., 2022. Greater Avalonia—latest Ediacaran-Ordovician "peribaltic" terrane bounded by continental margin prisms ("Ganderia", Harlech Dome, Meguma): review, tectonic implications, and paleogeography. Earth Sci. Rev. 224, 103863 https://doi.org/10.1016/j.earscirev.2021.103863.
Landing, E., 1996. Avalon: insular continent by the latest Precambrian. In: Nance, R.D., Thompson, M.D., (Eds.), Avalonian and Related Peri-Gondwanan Terranes of the Circum-North Atlantic: Boulder, Colorado, Geological Society of America Special Paper 304, pp. 29–63. https://doi.org/10.1130/0-8137-2304-3.29.
Matthews, J.J., Liu, A.G., Yang, C., McIlroy, D., Levell, B., Condon, D., 2021. A chronostratigraphic framework for the rise of the Ediacaran macrobiota: new constraints from Mistaken Point Ecological Reserve, Newfoundland. Geol. Soc. Am. Bull. 133, 612–624. https://doi.org/10.1130/B35646.1.
McClelland, W.C., Strauss, J.V., Gilotti, J.A., Colpron, M., 2023. Paleozoic evolution of the northern Laurentian margin: evaluating links between the Caledonian, Ellesmerian, and Cordilleran orogens. In: Whitmeyer, S.J., Williams, M.L., Kellett, D. A., Tikoff, B., (Eds.), Laurentia: Turning Points in the Evolution of a Continent: Geological Society of America Memoir 220, pp. 605–633. https://doi.org/10.1130/2022.1220(30).
McClelland, W.C., Strauss, J.V., Colpron, M., Gilotti, J.A., Faehnrich, K., Malone, S.J., Gehrels, G.E., Macdonald, F.A., Oldow, J.S., 2021. 'Taters versus Sliders: evidence for a long-lived history of strike-slip displacement along the Canadian Arctic Transform System (CATS). GSA Today 31, 4–11. https://doi.org/10.1130/GSATG500A.1.
McGee, B., Collins, A.S., Trindade, R.I.F., Payne, J., 2015. Age and provenance of the Cryogenian to Cambrian passive margin to foreland basin sequence of the northern Paraguay belt, Brazil. Geol. Soc. Am. Bull. 127, 76–86. https://doi.org/10.1130/B30842.1.
Meert, J.G., Torsvik, T.H., 2003. The making and unmaking of a supercontinent: Rodinia revisited. Tectonophysics 375, 261–288. https://doi.org/10.1016/S0040-1951(03)00342-1.
Miller, H.G., 1983. A geophysical interpretation of the geology of Conception Bay, Newfoundland. Can. J. Earth Sci. 20, 1421–1433. https://doi.org/10.1139/e83-128.
Mills, A.J., Dunning, G.R., Sandeman, H.A., 2021. Lithogeochemical, isotopic, and U-Pb (zircon) age constraints on arc to rift magmatism, northwestern and central Avalon terrane, Newfoundland, Canada: implications for local lithostratigraphy. Can. J. Earth Sci. 58, 332–354. https://doi.org/10.1139/cjes-2019-0196.

Mills, A.J., Calon, T., Peddle, C., 2016. Preliminary investigations into the structural geology of the Bonavista Peninsula, northeast Newfoundland: Current Research, Newfoundland and Labrador Department of Natural Resources, Geological Survey Report 16-1, p. 153-171.

Murphy, J.B., 2002. Geochemistry of the Neoproterozoic metasedimentary Gamble Brook Formation, Avalon terrane, Nova Scotia: evidence for a rifted-arc environment along the West Gondwanan margin of Rodinia. J. Geol. 110, 407–419. https://doi.org/10.1086/340630.

Murphy, J.B., Nance, R.D., 1989. Model for the evolution of the Avalonian-Cadomian belt. Geology 17, 735–738. https://doi.org/10.1130/0091-7613(1989)017<0735:MFTEOT>2.3.CO;2.

Murphy, J.B., Dostal, J., Keppie, J.D., 2008b. Neoproterozoic-Early Devonian magmatism in the Antigonish Highlands, Avalon terrane, Nova Scotia: tracking the evolution of the mantle and crustal sources during evolution of the Rheic Ocean. Tectonophysics 461, 181–201. https://doi.org/10.1016/j.tecto.2008.02.003.

Murphy, J.B., Keppie, J.D., Dostal, J., Hynes, A.J., 1990. The geochemistry and petrology of the late Precambrian Georgeville Group: a volcanic arc-rift succession in the Avalon terrane of Nova Scotia. In: D'Lemos, R.S., Strachan, R.A., Topley, C.G., (Eds.), The Cadomian Orogeny: Geological Society of London Special Publication 51, pp. 383–393. https://doi.org/10.1144/GSL.SP.1990.051.01.25.

Murphy, J.B., Keppie, J.D., Dostal, J., Nance, R.D., 1999. Neoproterozoic-early Paleozoic evolution of Avalonia. In: Ramos, V.A., Keppie, J.D., (Eds.), Laurentian-Gondwana Connections Before Pangea: Boulder, Colorado, Geological Society of America Special Paper 336, pp. 253–266. https://doi.org/10.1130/0-8137-2336-1.253.

Murphy, J.B., Strachan, R.A., Nance, R.D., Parker, K.D., Fowler, M.B., 2000. Proto-Avalonia: a 1.2-1.0 Ga tectonothermal event and constraints for the evolution of Rodinia. Geology 28, 1071–1074. https://doi.org/10.1130/0091-7613(2000)28<1071:PAGTEA>2.0.CO;2.

Murphy, J.B., Nance, R.D., Keppie, J.D., Dostal, J., 2019, Role of Avalonia in the development of tectonic paradigms. In: Wilson, R.W., Houseman, G.A., McCaffrey, K.J.W., Dore, A.G., Buiter, S.J.H., (Eds.), Fifty Years of the Wilson Cycle Concept in Plate Tectonics: Geological Society of London Special Publication 470, pp. 265–287. https://doi.org/10.1144/SP470.12.

Murphy, J.B., Nance, R.D., Wu, L., 2023. The provenance of Avalonia and its tectonic implications: a critical reappraisal. In: Hynes, A.J., Murphy, J.B., (Eds.), The Consummate Geoscientist: A Celebration of the Career of Maarten de Wit. Geological Society of London Special Publications 531. https://doi.org/10.1130/G36194.1.

Murphy, J.B., Pisarevsky, S.A., Nance, R.D., Keppie, J.D., 2004. Neoproterozoic-Early Paleozoic evolution of peri-Gondwanan terranes: implications for Laurentia-Gondwana connections. Int. J. Earth Sci. 93, 659–682. https://doi.org/10.1007/s00531-004-0412-9.

Murphy, J.B., McClausland, P.J.A., O'Brien, S.J., Pisarevsky, S., Hamilton, M.A., 2008a. Age, geochemistry and Sm-Nd isotopic signature of the 0.76 Ga Burin Group: compositional equivalent of Avalonian basement? Precambr. Res. 165, 37–48. https://doi.org/10.1016/j.precamres.2008.05.006.

Murphy, J.B., van Staal, C.R., Collins, W.J., 2011. A comparison of the evolution of arc complexes in Paleozoic interior and peripheral orogens: Speculations on geodynamic correlations. Gondw. Res. 19, 812–827. https://doi.org/10.1016/j.gr.2010.11.019.

Murphy, J.B., Pisarevsky, S., Nance, R.D., 2013. Potential geodynamic relationships between the development of peripheral orogens along the northern margin of Gondwana and the amalgamation of West Gondwana. Mineral. Petrol. 107, 635–650. https://doi.org/10.1007/s00710-012-0207-9.

Myrow, P.M., 1995. Neoproterozoic rocks of the Newfoundland Avalon Zone. Precambr. Res. 73, 123–136. https://doi.org/10.1016/0301-9268(94)00074-2.

Nance, R.D., Murphy, J.B., Strachan, R.A., Keppie, J.D., Gutierrez-Alonso, G., Fernandez-Suarez, J., Quesada, C., Linnemann, U., D'Lemos, R., Pisarevsky, S.A., 2008. Neoproterozoic-early Paleozoic tectonostratigraphy and paleogeography of the peri-Gondwanan terranes: Amazonian v. West African connections. In: Ennih, N., Liegeois, J.-P., (Eds.), The Boundaries of the West African Craton, Geological Society of London Special Publication 297, pp. 345–383. https://doi.org/10.1144/SP297.17.

Nance, R.D., Murphy, J.B., Keppie, J.D., 2002. Cordilleran model for the evolution of Avalonia. Tectonophysics 352, 11–32. https://doi.org/10.1016/S0040-1951(02)00187-7.

O'Brien, S.J., King, A.F., 2004. Late Neoproterozoic to earliest Paleozoic stratigraphy of the Avalon zone in the Bonavista Peninsula: Current Research, Newfoundland Department of Mines and Energy, Geological Survey of Newfoundland and Labrador, Report 04-1, p. 213-224.

O'Brien, S.J., Dunning, G.R., Dube, B., O'Driscoll, C.F., Sparkes, B., Israel, S., Ketchum, J., 2001. New insights into the Neoproterozoic geology of the central Avalon Peninsula (parts of NTS map areas 1N/6, 1N/7, and 1N/3). Current Research, Newfoundland Department of Mines, eastern Newfoundland, pp. 193–205. Report 2001–1,.

O'Brien, S.J., O'Driscoll, C.F., Greene, B.A., Tucker, R.D., 1995. Pre-Carboniferous geology of the Connaigre Peninsula and the adjacent coast of Fortune Bay, southern Newfoundland: Current Research, Department of Natural Resources, Geological Survey of Newfoundland and Labrador, Report 95-1, pp. 267–297.

O'Brien, S.J., O'Brien, B.H., Dunning, G.R., Tucker, R.D., 1996. Late Neoproterozoic Avalonian and related peri-Gondwanan rocks of the Newfoundland Appalachians. In: Nance, R.D., Thompson, M.D., (Eds.), Avalonian and Related Peri-Gondwanan Terranes of the Circum-North Atlantic: Boulder, Colorado, Geological Society of America Special Paper 304, pp. 9–28. https://doi.org/10.1130/0-8137-2304-3.9.

Papezik, V.S., 1972. Burial metamorphism of late Precambrian sediments near St. John's, Newfoundland. Can. J. Earth Sci. 9, 1568–1572. https://doi.org/10.1016/j.marpetgeo.2022.105960.

Papezik, V.S., 1973. Detrital garnet and muscovite in late Precambrian sandstone near St. John's, Newfoundland, and their significance. Can. J. Earth Sci. 10, 430–432. https://doi.org/10.1139/e73-04.

Papezik, V.S., 1974. Prehnite-pumpellyite facies metamorphism of late Precambrian rocks of the Avalon Peninsula, Newfoundland. Can. Mineral. 12, 463–468.

Paszkowski, M., Budzyn, B., Mazur, S., Slama, J., Shumlyanskyy, L., Srodon, J., Dhuime, B., Kedzior, A., Liivamagi, S., Pisarzowska, A., 2019. Detrital zircon U-Pb and Hf constraints on provenance and timing of deposition of the Mesoproterozoic to Cambrian sedimentary cover of the East European craton v. 331, 105352. https://doi.org/10.1016/j.precamres.2019.105352.

Paton, C., Hellstrom, J., Paul, B., Woodhead, J., Hergt, J., 2011. Iolite: Freeware for the visualisation and processing of mass spectrometric data. J. Anal. At. Spectrom 26, 2508–2518. https://doi.org/10.1039/c1ja10172b.

Pease, V., 2021. Eastern Europe: The Timanian and Uralian Orogens: encyclopedia of Geology, 2nd edition. Elsevier, pp. 302–310.

Pease, V., Scott, R.A., 2009. Crustal affinities in the Arctic Uralides, northern Russia: significance of detrital zircon ages from Neoproterzoic and Palaeozoic sediments in Novaya Zemlya and Taimyr. J. Geol. Soc. Lond. 166, 517–527. https://doi.org/10.1144/0016-76492008-093.

Pe-Piper, G., Murphy, J.B., 1989. Geochemistry and tectonic setting of the late Precambrian Folly River Formation, Cobequid Highlands, Avalon Terrane, Nova Scotia: a continental rift within a volcanic-arc environment. Atl. Geol. 25, 143–151.

Pe-Piper, G., Piper, D.J.W., 1989. The upper Hadrynian Jeffers Group, Cobequid Highlands, Avalon zone of Nova Scotia: a back-arc volcanic complex. Geol. Soc. Am. Bull. 101, 364–376. https://doi.org/10.1130/0016-7606(1989)101<0364:TUHJGC>2.3.CO;2.

Pe-Piper, G., Piper, D.J.W., 1998. Geochemical evolution of Devonian-Carboniferous igneous rocks of the Magdalen basin, eastern Canada: Pb- and Nd-isotope evidence for mantle and lower crustal sources. Can. J. Earth Sci. 35, 201–221. https://doi.org/10.1139/e97-106.

Peron-Pinvidic, G., Manatschal, G., 2010. From microcontinents to extensional allochthons: witnesses of how continents rift and break apart? Pet. Geosci. 16, 189–197. https://doi.org/10.1144/1354-079309-903.

Petrus, J.A., Kamber, B.S., 2012. VizualAge: a novel approach to laser ablation ICP-MS U-Pb geochronology data reduction. Geostand. Geoanal. Res. 36, 247–270. https://doi.org/10.1111/j.1751-908X.2012.00158.x.

Pollock, J.C., Sylvester, P.J., Barr, S.M., 2015. Lu-Hf zircon and Sm-Nd whole-rock isotope constraints on the extent of juvenile arc crust in Avalonia: examples from Newfoundland and Nova Scotia, Canada. Can. J. Earth Sci. 52, 161-181. https://doi.org/10.1139/cjes-2014-0157.

Pollock, J.C., Barr, S.M., van Rooyen, D., White, C.E., 2022. Insights from Lu-Hf zircon isotopic data on the crustal evolution of Avalonia and Ganderia in the northern Appalachian orogen. In: Kuiper, Y.D., Murphy, J.B., Nance, R.D., Strachan, R.A., Thompson, M.D., (Eds.), New Developments in the Appalachian-Variscan Orogen: Boulder, Colorado, Geological Society of America Special Paper 554, pp. 173-207. https://doi.org/10.1130/2021.2554(08).

Pollock, J.C., Hibbard, J.P., Sylvester, P.J., 2009. Early Ordovician rifting of Avalonia and birth of the Rheic Ocean: U-Pb detrital zircon constraints from Newfoundland. J. Geol. Soc. Lond. 166, 501–515. https://doi.org/10.1144/0016-76492008-088.

Pu, J., Bowring, S.A., Ramezani, J., Myrow, P., Raub, T.D., Landing, E., Mills, A., Hodgin, E., Macdonald, F.A., 2016. Dodging snowballs: geochronology of the Gaskiers glaciation and the first appearance of the Ediacaran biota. Geology 44, 955–958. https://doi.org/10.1130/G38284.1.

Reusch, D.N., Holm-Denoma, C.S., Slack, J.F., 2018. U-Pb zircon geochronology of Proterozoic and Paleozoic rocks, North Islesboro, coastal Main (USA): links to West Africa and Penobscottian orogenesis in southeastern Ganderia? Atl. Geol. 54, 189–221. https://doi.org/10.4138/atlgeol.2018.007.

Robert, B., Domeier, M., Jakob, J., 2021. On the origins of the Iapetus Ocean. Earth Sci. Rev. v. 221, 103791 https://doi.org/10.1016/j.earscirev.2021.103791.

Roberts, D., Olovyanishnikov, V., 2004. In: Gee, D.G., Pease, V. (Eds.), The Neoproterozoic Timanide Orogen of Eastern Baltica, 30. Geological Society of London Memoir, pp. 47–57. https://doi.org/10.1144/GSL.MEM.2004.030.01.05.

Rose, E.R., 1952. Torbay map area, Newfoundland: Geological Survey of Canada. Memoir 265, 64 pp.

Salminen, J., Lehtonen, E., Mertanen, S., Pesonen, L.J., Elming, S.-A., Luoto, T., 2021. The Precambrian drift history and paleogeography of Baltica. In: Pesonen, L.J., Salminen, J., Evans, D.A.D., Elming, S.-A., Veikkolaninen, T., (Eds.), Ancient Supercontinents and the Paleogeogeography of Earth: Elsevier, pp.155-205. https://doi.org/10.1016/B978-0-12-818533-9.00015-1.

Samson, S.D., Barr, S.M., White, C.E., 2000. Nd isotopic characteristics of terranes within the Avalon zone, southern New Brunswick. Can. J. Earth Sci. 37, 1039–1052. https://doi.org/10.1139/e00-015.

Satkoski, A.M., Barr, S.M., Samson, S.D., 2010. Provenance of late Neoproterozoic and Cambrian sediments in Avalonia: Constraints from detrital zircon ages and Sm-Nd isotopic compositions in southern New Brunswick, Canada. J. Geol. 118, 187-200. https://doi.org/10.1086/649818.

Saylor, J.E., Sundell, K.E., 2016. Quantifying comparison of large detrital geochronology data sets. Geosphere 12, 203–220. https://doi.org/10.1130/GES01237.1.

Saylor, J.E., Jordan, J.C., Sundell, K.E., Wang, X., Wang, S., Deng, T., 2018. Topographic growth of the Jishi Shan and its impact of basin and hydrology evolution, NE Tibetan Plateau. Basin Res. 30, 544–563. https://doi.org/10.1111/bre.12264.

Saylor, J.E., Sundell, K.E., Sharman, G.R., 2019. Characterizing sediment sources by non-negative matrix factorization of detrital geochronological data. Earth Planet. Sci. Lett. 512, 46–58. https://doi.org/10.1016/j.epsl.2019.01.044.

Scarrow, J.H., Pease, V., Fleutelot, C., Dushin, V., 2001. The late Neoproterozoic Enganepe ophiolite, Polar Urals, Russia: an extension of the Cadomian arc? Precambr. Res. 110, 255–275. https://doi.org/10.1016/S0301-9268(01)00191-7.

Schofield, D., Millar, I.L., Wilby, P.R., Evans, J.A., 2010. A new, high precision U-Pb date from the oldest known rocks in southern Britian. Geol. Mag. 147, 145–150. https://doi.org/10.1017/S001675680999063X.

Severson, A.R., Kuiper, Y.D., Eby, G.N., Lee-H.-Y., Hepburn, J.C., 2022. New detrital zircon U-Pb ages and Lu-Hf isotopic data from metasedimentary rocks along the western boundary of the composite Avalon terrane in the southeastern New England Appalachians. In: Kuiper, Y.D., Murphy, J.B., Nance, R.D., Strachan, R.A., Thompson, M.D., (Eds.), New Developments in the Appalachian-Variscan Orogen: Boulder, Colorado, Geological Society of America Special Paper 554, pp. 73-91. https://doi.org/10.1130/2021.2554(04).

Sharman, G.R., Malkowski, M.A., 2020. Needles in a haystack: detrital zircon U-Pb ages and the maximum depositional age of modern global sediment. Earth Sci. Rev. 203, 103109 https://doi.org/10.1016/j.earscirev.2020.103109.

Shumlyanskyy, L., Hawkesworth, C., Dhuime, B., Billstrom, K., Claesson, S., Storey, C., 2015. $^{207}Pb/^{206}Pb$ ages and Hf isotope composition of zircons from sedimentary rocks of the Ukrainian shield: crustal growth of the southwestern part of East European craton from Archaean to Neoproterozoic. Precambr. Res. 260, 39–54. https://doi.org/10.1016/j.precamres.2015.01.007.

Skipton, D.R., Dunning, G.R., Sparkes, G.W., 2013. Late Neoproterozoic arc-related magmatism in the Horse Cove complex, eastern Avalon zone, Newfoundland. Can. J. Earth Sci. 50, 462–482. https://doi.org/10.1139/cjes-2012-0090.

Söderlund, U., Patchett, P.J., Vervoort, J.D., Isachsen, C.E., 2004. The ^{176}Lu decay constant determined by Lu-Hf and U-Pb isotope systematics of Precambrian mafic intrusions. Earth Planet. Sci. Lett. 219, 311–324. https://doi.org/10.1016/S0012 821X(04)00012-3.

Sparkes, G., Beranek, L.P., Mills, A., 2021. From the roof to the basement: a tour of structures, sedimentary rocks, and epithermal systems of the northeastern Avalon: geological association of canada-newfoundland and labrador section. Field Trip Guide 28, pp.

Stewart, D.B., Tucker, R.D., Ayuso, R.A., Lux, D.R., 2001. Minimum age of the neoproterozoic seven hundred acre island formation and the tectonic setting of the islesboro formation, Islesboro block, Maine. Atlantic Geol. 37, 41–59.

Strong, D.F., Dostal, J., 1980. Dynamic melting of Proterozoic upper mantle: evidence from rare earth elements in oceanic crust of eastern Newfoundland. Contrib. Miner. Petrol. 72, 165–173. https://doi.org/10.1007/BF00399476.

Sundell, K.E., Saylor, J.E., 2021. Two-dimensional quantitative comparison of density distributions in detrital geochronology and geochemistry. Geochem. Geophys. Geosyst. 22, e2020GC009559. https://doi.org/10.1029/2020GC009559.

Sundell, K., Saylor, J.E., Pecha, M., 2019. Provenance and recycling of detrital zircons from Cenozoic Altiplano strata and the crustal evolution of western South America from combined U-Pb and Lu-Hf isotopic analysis. In: Horton, B., Folguera, A., (Eds.), Andean Tectonics. Amsterdam, Elsevier, 3p. 63–397. https://doi.org/10.1016/B978-0-12-816009-1.00014-9.

Sylvester, P.J., 2012. Use of the mineral liberation analyzer (MLA) for mineralogical studies of sediments and sedimentary rocks. In: Sylvester, P. (Ed.), Quantitative Mineralogy and Microanalysis of Sediments and Sedimentary Rocks: Mineralogical Association of Canada Short Course 42. Quebec, Canada, pp. 1–16.

Thompson, M.D., Barr, S.M., Grunow, A.M., 2012. Avalonian perspectives on Neoproterozoic paleogeography: Evidence from Sm-Nd isotope geochemistry and detrital zircon geochronology in SE New England, USA. Geol. Soc. Am. Bull. 124, 517–531. https://doi.org/10.1130/B30529.1.

Thompson, M.D., Barr, S.M., Pollock, J.C., 2022. Evolving views of West Avalonia: Perspectives from southeastern New England, USA. In: Kuiper, Y.D., Murphy, J.B., Nance, R.D., Strachan, R.A., Thompson, M.D., (Eds.), New Developments in the Appalachian-Variscan Orogen: Boulder, Colorado, Geological Society of America Special Paper 554, pp. 47-72. https://doi.org/10.1130/2022.2554(03).

Thompson, M.D., Ramezani, J., Crowley, J.L., 2014. U-Pb zircon geochronology of Roxbury Conglomerate, Boston basin, Massachusetts: tectono-stratigraphic implications for Avalonia in and beyond SE New England. Am. J. Sci. 314, 1009–1040. https://doi.org/10.2475/06.2014.02.

van Staal, C.R., Barr, S.M., 2012. Lithospheric architecture and tectonic evolution of the Canadian Appalachians and associated Atlantic margin. In: Percival, J.A., Cook, F.A., Clowes, R.M., Tectonic Styles in Canada: the LITHOPROBE perspective: Geological Association of Canada Special Paper 49, pp. 41-95.

van Staal, C.R., Dewey, J.F., Mac Niocaill, C., McKerrow, W.S., 1998. The Cambrian-Silurian tectonic evolution of the northern Appalachians and British Caledonides: history of a complex, west and southwest-Pacific-type segment of Iapetus. In: Blundell, D.J., Scott, A.C., (Eds.), Lyell: The Past is the Key to the Present: Geological Society of London Special Publication 143, pp. 199–242. https://doi.org/10.1144/GSL.SP.1998.143.01.17.

van Staal, C.R., Whalen, J.B., Valverde-Vaquero, P., Zagorevski, A., Rogers, N., 2009. Pre-Carboniferous, episodic accretion-related, orogenesis along the Laurentian margin of the northern Appalachians. In: Murphy, J.B., Keppie, J.D., Hynes, A.J., (Eds.), Ancient Orogens and Modern Analogues: Geological Society of London Special Publications 327, pp. 271–316. https://doi.org/10.1144/SP327.1.

van Staal, C.R., Barr, S.M., McClausland, P.J.A., Thompson, M.D., White, C.E., 2021a. Tonian-Ediacaran tectonomagmatic evolution of West Avalonia and its Ediacaran-early Cambrian interactions with Ganderia: an example of complex terrane transfer due to arc-arc collision? In: Murphy, J.B., Strachan, R.A., Quesada, C., (Eds.), Pannotia to Pangaea: Neoproterozoic and Paleozoic Orogenic Cycles in the Circum-Atlantic Region: Geological Society of London Special Publications 503, pp. 143–167. https://doi.org/10.1144/SP503-2020-23.

van Staal, C.R., Barr, S.M., Waldron, J.W.F., Schofield, D.I., Zagorevski, A., White, C.E., 2021b. Provenance and Paleozoic tectonic evolution of Ganderia and its relationships with Avalonia and Megumia in the Appalachian-Caledonide orogen. Gondwana Res. 98, 212–243. https://doi.org/10.1016/j.gr.2021.05.025.

Vermeesch, P., 2018. Disimiliarity measures in detrital geochronology. Earth Sci. Rev. 178, 310–321. https://doi.org/10.1016/j.earscirev.2017.11.02.

Vermeesch, P., 2021. Maximum depositional age estimation revisited. Geosci. Front. 12, 843–850. https://doi.org/10.1016/j.gsf.2020.08.008.

Vervoort, J.D., Blichert-Toft, J., 1999. Evolution of the depleted mantle: Hf isotope evidence from juvenile rocks through time. Geochim. Cosmochim. Acta 63, 533–556. https://doi.org/10.1016/S0016-7037(98)00274-9.

Vervoort, J.D., Patchett, P.J., Blichert-Toft, J., Albarede, F., 1999. Relationships between Lu-Hf and Sm-Nd isotopic systems in the global sedimentary system. Earth Planet. Sci. Lett. 168, 79–99. https://doi.org/10.1016/S0012-821X(99)00047-3.

Waldron, J.W.F., Schofield, D.I., Murphy, J.B., Thomas, C.W., 2014. How was the Iapetus Ocean infected with subduction? Geology 42, 1095–1098. https://doi.org/10.1130/G36194.1.

Waldron, J.W.F., Schofield, D.I., Pearson, G., Sarkar, C., Luo, Y., Dokken, R., 2019. Detrital zircon characterization of early Cambrian sandstones from East Avalonia and SE Ireland: implications for terrane affinities in the peri-Gondwanan Caledonides. Geol. Mag. 156, 1217–1232. https://doi.org/10.1017/S0016756818000407.

White, C.E., Barr, S.M., Hamilton, M.A., Murphy, J.B., 2021. Age and tectonic setting of Neoproterozoic granitoid rocks, Antigonish Highlands, Nova Scotia, Canada: implications for Avalonia in the northern Appalachian orogen. Can. J. Earth Sci. 58, 396–412. https://doi.org/10.1139/cjes-2020-0110.

White, C.E., Barr, S.M., Crowley, J.L., van Rooyen, D., MacHattie, T.G., 2022. U-Pb zircon ages and Sm-Nd isotopic data from the Cobequid Highlands, Nova Scotia, Canada: New contributions to understanding the Neoproterozoic geologic history of Avalonia. In: Kuiper, Y.D., Murphy, J.B., Nance, R.D., Strachan, R.A., Thompson, M. D., (Eds.), New Developments in the Appalachian-Caledonian-Variscan Orogen: Boulder, Colorado, Geological Society of America Special Paper 554, pp. 135–172. https://doi.org/10.1130/2021.2554(07).

Williams, H., 1979. Appalachian orogen in Canada. Can. J. Earth Sci. 16, 792–807. https://doi.org/10.1139/e79-070.

Williams, H., O'Brien, S.J., King, A.F., Anderson, M.M., 1995. Avalon Zone-Newfoundland (Chapter 3). In: Williams, H., (Ed.), Geology of the Appalachian-Caledonian Orogen in Canada and Greenland: Geological Society of America, The Geology of North America, vol. F-1, pp. 226-237. https://doi.org/10.1130/DNAG-GNA-F1.45.

Williams, H., King, A.F., 1979. Trepassey map area, newfoundland: geological survey of canada. Memoir 389, 24 pp.

Willner, A.P., Barr, S.M., Gerdes, A., Massonne, H.-J., White, C.E., 2013. Origin and evolution of Avalonia: evidence from U-Pb and Lu-Hf isotopes in zircon from the Mira terrane, Canada, and the Stavelot-Venn Massif, Belgium. J. Geol. Soc. 170, 769–784. https://doi.org/10.1144/jgs2012-152.

Willner, A.P., Gerdes, A., Massonne, H.-J., van Staal, C.R., Zagorevski, A., 2014. Crustal evolution of the northeast Laurentian margin and the peri-Gondwanan microcontinent Ganderia prior to and during closure of the Iapetus Ocean: detrital zircon U-Pb and Hf isotope evidence from Newfoundland. Geosci. Can. 41, 345–364. https://doi.org/10.12789/geocanj.2014.41.046.

Willner, A.P., Gopon, M., Glodny, J., Puchkov, V.N., Schertl, H.-S., 2019. Timanide (Ediacaran-Early Cambrian) metamorphism at the transition from eclogite to amphibolite facies in the Beloretsk complex, SW-Urals, Russia. J. Earth Sci. 30, 1144–1165. https://doi.org/10.1007/s12583-019-1249-2.

Wissink, G.K., Wilkinson, B.H., Hoke, G.D., 2018. Pairwise sample comparisons and multidimensional scaling of detrital zircon ages with examples from the North American platform, basin, and passive margin settings. Lithosphere 10, 478–491. https://doi.org/10.1130/L700.1.

Zhang, W., Roberts, D., Pease, V., 2015. Provenance characteristics and regional implications of Neoproterozoic, Timanian-margin successions and basal Caledonian nappe in northern Norway. Precambr. Res. 268, 153–167. https://doi.org/10.1016/j.precamres.2015.07.006.